



THE OSSIFIED BRAINCASE AND CEPHALIC OSTEODERMS OF *SHINISAURUS CROCODILURUS* (SQUAMATA, SHINISAURIDAE)

Gabe S. Bever, Christopher J. Bell, and Jessica A. Maisano

ABSTRACT

We review the literature and provide a detailed description of the braincase, cephalic osteoderms, and the inner ear cavity of the rare Southeast Asian lizard *Shinisaurus crocodilurus*. In addition to standard dry skeletal preparations, we used X-ray computed tomography scans of an adult and juvenile specimen to provide novel illustrations and digital animations of its anatomical systems. We provide the first detailed description and illustration of the orbitosphenoids, cephalic osteoderms, and inner ear passages in *S. crocodilurus*, clarify the presence or absence of previously reported anatomical features of the braincase, and provide preliminary observations on morphological change of the braincase through ontogeny. Orbitosphenoids are present and ossified in *S. crocodilurus* at a relatively early stage of postnatal development. A fully developed and ossified parasphenoid rostrum is present in our youngest dried specimen, but appears to be reduced or broken in many adult specimens. The osteoderms of adult *S. crocodilurus* are robust and widely distributed across the dorsal surface of the head, but they do not co-ossify with underlying dermal bones. Osteoderms are absent in our juvenile specimens. Calcified endolymph is present in both adult and juvenile specimens, but is more extensive in the juvenile. Our preliminary observations suggest that ontogenetic change is an important source of variation in *S. crocodilurus*.

KEY WORDS: *Shinisaurus*; crocodile lizard; Krokodilschwanz-Höckerechse; osteology; anatomy; braincase; osteoderms, inner ear

Gabe S. Bever. Department of Geological Sciences, Jackson School of Geosciences, The University of Texas at Austin, Austin, Texas 78712 gbever@mail.utexas.edu

Christopher J. Bell. Department of Geological Sciences, Jackson School of Geosciences, The University of Texas at Austin, Austin, Texas 78712 cjbelle@mail.utexas.edu

Jessica A. Maisano. Department of Geological Sciences, Jackson School of Geosciences, The University of Texas at Austin, Austin, Texas 78712 maisano@mail.utexas.edu

PE Article Number: 8.1.4

Copyright: Society of Vertebrate Paleontology May 2005

Submission: 23 July 2004. Acceptance: 13 April 2005

INTRODUCTION

The Chinese crocodile lizard, *Shinisaurus crocodilurus* Ahl, is an enigmatic anguimorph lizard that today is known only to inhabit portions of southeastern China and northeastern Vietnam. In this paper, we expand on the relatively limited history of anatomical investigations on *S. crocodilurus* by providing the first detailed description of the braincase, cephalic osteoderms, and inner ear cavities. These descriptions largely are based on digital data derived from X-ray computed tomography, a nondestructive technique well suited for studying such rare and scientifically important specimens.

Shinisaurus crocodilurus is a relatively small-bodied (up to 397 mm body length) anguimorph lizard that occupies mountain stream habitats characterized by humid climate with annual rainfall up to 2 m (Shen and Li 1982, 1987). In China, *S. crocodilurus* was found between 200 and 1,500 m elevation (Zhao and Adler 1993; Zhao et al. 1999) in Guangxi Province between 23°25' to 24°45' N latitude and 110°48' to 110°00' E longitude (Zhao et al. 1999). Until recently, the species was thought to be restricted to this limited area of southeastern China. A newly discovered population in Quang Ninh Province of northeastern Vietnam was reported by Quyet and Ziegler (2003). Specimens from that new population were collected between 600 and 800 m elevation in habitats along stream banks, but no natural history data are available.

The species is ovoviviparous (Shen and Li 1982, 1987; Zhang and Tang 1985; Mägdefrau 1987; Zhao et al. 1999), and breeds in July and August in the wild (Zhang and Tang 1985; Zhang 1991) but at different times in captivity (Hofmann 2000). Individuals are largely diurnal, but generally do not engage in intensive activity (Zhao et al. 1999), spending long hours perched on rocks or branches above slow-moving streams and ponds (Zhao et al. 1999; Hofmann 2000). Relatively long periods of absolute immobility are apparently not uncommon in captivity (Sprackland 1989, 1995), and similar behavior in the wild earned the lizards the local common name "large sleeping serpent" (Zhao et al. 1999). When disturbed, individuals retreat to water for escape (Fan 1931; Quyet and Ziegler 2003); adults were observed to remain submerged for 10 to 20 minutes in the wild (Zhao et al. 1999; Quyet and Ziegler 2003), and in one case a captive lizard stayed underwater for six hours (Sprackland 1995).

Foraging activity in the wild is concentrated in early morning and in the evening. Diet in the wild includes dragonflies, aquatic beetle larvae, lepidopteran larvae, aquatic insects, grasshoppers,

small fish, tadpoles, and grass seeds (Fan 1931; Shen and Li 1982, 1987) and possibly worms, rice borers, cockroaches, and small, metamorphosed anurans (Zhao et al. 1999). Individuals congregate in winter months and hibernate in rock crevices or tree holes from late October through late March (Zeng and Zhang 2002).

The relatively rugged terrain inhabited by *S. crocodilurus* in China and Vietnam provides some measure of protection for populations, but also restricts enforcement of conservation laws. Specimens of *S. crocodilurus* were exported for the pet trade in Europe and the United States in great numbers in the mid 1980s (Mägdefrau 1987; Sprackland 1989). The species was listed in CITES Appendix II in January 1990 and now receives full State protection in several areas of China (Zhao et al. 1999). Habitat destruction and human predation reduced known Chinese population sizes to an estimated 3,000 individuals by 1999 (Zhao et al. 1999) with some populations reduced to fewer than 20 individuals (Zhang and Zeng 2002). Illegal logging threatens the newly discovered Vietnamese population (Quyet and Ziegler 2003).

Fortunately, many individuals who obtained imported specimens established captive breeding programs and produced several publications detailing various aspects of general biology and behavior, including: 1) courtship; 2) copulation; 3) gestation period; 4) thermal preferences; 5) agonistic behavior; 6) sexual dimorphism; 7) ontogenetic variation; and 8) variation in coloration (e.g., Wilke 1985, 1987; Mägdefrau 1987, 1997; Sprackland 1989, 1993, 1995; Gritis 1990; Thatcher 1990; Kudryavtsev and Wasiljew 1991; Grychta 1993; Kudryavtsev and Vassilyev 1998; Hofmann 2000).

THE ANATOMY OF *SHINISAURUS*

For more than two decades following its original description in 1930, virtually nothing was known about the anatomy of *S. crocodilurus*. General descriptions of external scale counts and variation in coloration were provided by Fan (1931) and were accompanied by photographs of the ventral surface of the body, a lateral view of the anterior torso and head, and a lateral view of the tail. The first major anatomical contribution was that of McDowell and Bogert (1954). Their discussion centered on osteology (with additional comments on the tongue) but was based upon dissection of a single, skeletally immature specimen in the American Museum of Natural History (AMNH 44928). That same specimen served as the basis for the first description of masticatory muscles (Haas 1960; followed by subsequent papers detailing

additional observations by Haas 1973 and Rieppel 1980) and the eye (Underwood 1957, 1970). Subsequent papers addressed the vertebral column (Hecht and Costelli 1969), appendicular skeleton (Costelli and Hecht 1971), myology (Rieppel 1980; Huang 1992), brain and both cranial and spinal nerves (Hu 1980), liver and kidney enzymes (Zhao et al. 1980), digestive and urogenital systems (Zhang 1982), hemipenial morphology (Zhang 1986; Böhme 1988; Ziegler and Böhme 1997), optic nerve (Li and Wu 1988), microscopic anatomy of scales (Harvey 1993), karyotype (Zhang et al. 1996; Zhao et al. 1999), cellular ultrastructure (Zhang et al. 1996), mitochondrial DNA sequence (Macey et al. 1999), and protein electrophoresis (Wei et al. 2000). An overview of the general anatomy of *S. crocodilurus* was provided by Zhang and Cao (1984a, 1984b) and a more detailed treatment by Zhang (1991); both of these works are in Chinese, but the latter provides a brief English summary.

In this paper, we focus on two anatomical systems of *S. crocodilurus* that have as yet received inadequate attention: the detailed morphology of the braincase and the cephalic osteodermal armor. Our discussion of the braincase is augmented by description of some aspects of the inner ear structure. When we first conceived this project, our intention was to provide a complete and detailed review of the cranial osteology of *S. crocodilurus*. This became unnecessary upon the recent publication of an excellent study by Jack Conrad (2004). That paper is by far the most complete contribution to the osteology of *S. crocodilurus*. Additional important works discussed and/or illustrated the skull (McDowell and Bogert 1954; Rieppel 1980; Wu and Huang 1986; Zhang 1991), dentition (McDowell and Bogert 1954; Wu and Huang 1986; Zhang 1991), hyoid (McDowell and Bogert 1954; Wu and Huang 1986; Zhang 1991), vertebral column (Wu and Huang 1986; Zhang 1991), pectoral girdle (McDowell and Bogert 1954; Costelli and Hecht 1971; Wu and Huang 1986; Zhang 1991), pelvic girdle (Costelli and Hecht 1971; Wu and Huang 1986; Zhang 1991), limb skeleton (Costelli and Hecht 1971), and scleral ossicles (Underwood 1957, 1970; Zhang 1991).

FOSSIL RECORD

There is no fossil record for *S. crocodilurus*, and Asian fossils potentially referable to Shinisauridae are few. *Hemishinisaurus latifrons* is known from a broken frontal and prefrontals and the fragmentary tip of a maxilla. These specimens were described and illustrated by Li (1991) who placed

them in "Xenosauridae." The anterior dentition in Li's (1991, figure 2B) appears to have acrodont implantation, suggesting a more likely affinity with Acrodonta.

Disarticulated dentaries referred to *Oxia karakalpakiensis* from the Cretaceous of Uzbekistan were assigned to "Xenosauridae" by Nesson and Gao (1993), but in a subsequent detailed analysis Gao and Nesson (1998) recognized that definitive placement of these elements was problematic. Although Alifanov (2000) retained *Oxia* in "Shinisauridae," its phylogenetic position is best considered uncertain (Gao and Norell 1998). Additional undescribed specimens from the Early Cretaceous Höövör locality in Mongolia were tentatively referred to Shinisauridae by Alifanov (2000).

The phylogenetic position of *Carusia intermedia* was uncertain for many years. It was initially considered to be of scincomorphan affinity (Borsuk-Bialynicka 1985, 1987; Gao and Hou 1996), a hypothesis maintained by Alifanov (2000). A possible relationship with Xenosauridae was acknowledged in the original description (Borsuk-Bialynicka 1985) and appears to have been accepted a few years later (Borsuk-Bialynicka 1991a, 1991b). The recovery of numerous well-preserved specimens of *Carusia intermedia* was reported by Gao and Norell (1998), and their phylogenetic analysis supports a clade (Carusioidea) that minimally includes *Carusia* (basal), *Xenosaurus*, and *S. crocodilurus*. The North American lizards *Exostinus* and *Restes* also are likely members of this clade (reviews of their fossil record and hypotheses of relationship were summarized by Gauthier [1982] and Gao and Norell [1998]).

More recently, an exquisitely preserved fossil from the Green River Formation in Wyoming (USA) was discovered. Preliminary notice and discussion of the specimen was provided by Conrad (2002) who indicated that its skeleton is remarkably similar to that of *S. crocodilurus*.

MATERIALS AND METHODS

The heads of two alcohol-preserved specimens of *S. crocodilurus* were scanned at The University of Texas at Austin High-Resolution X-ray Computed Tomography (CT) Facility (UTCT). The first specimen (Field Museum of Natural History, FMNH 215541; 136.5 mm snout-vent length [SVL]) is an adult collected from Jinxin County, Guangxi Province, China, in June 1978. The original data set of the adult consists of 465 CT slices taken along the coronal or transverse axis with both a slice thickness and interslice spacing of 78.4 μm . The field of reconstruction is 30.0 mm with an

image resolution of 1024 x 1024 pixels, resulting in an interpixel spacing of 29.3 μm . The second specimen (Texas Natural History Collection, Texas Memorial Museum, TNHC 62987; 59.1 mm SVL) is a juvenile specimen for which no locality information is known. The original data set of the juvenile consists of a total of 516 coronal CT slices, with both the slice thickness and interslice spacing equaling 29.0 μm . The field of reconstruction is 12.5 mm with an image resolution of 512 x 512 pixels, resulting in an interpixel spacing of 24.4 μm . The difference in resolution between the juvenile and adult datasets is due to technological upgrades of the UTCT scanner between April 2000, when the juvenile was scanned, and March 2004, when the adult was scanned. That difference in resolution, as well as the lesser degree of ossification, results in poorer quality of the juvenile dataset.

The original coronal CT slices for both juvenile and adult were resliced along the horizontal and sagittal planes and then used to create three-dimensional (3-D) digital reconstructions of the skulls. The skulls were then segmented into constituent parts (e.g., dermatocranium, splanchnocranium, neurocranium) using VG Studio Max[®] (Volume Graphics). We performed additional segmentation on the braincase of both the juvenile and the adult so that individual bones could be studied and figured in isolation. We also rendered a digital endocast of the cavities of the inner ear of the adult to study its structure.

Certain areas (e.g., portions of the prootic covering the anterior semicircular canal, portions of the parasphenoid rostrum) appear to be absent in the three-dimensional reconstructions. This is because the grayscale (= density) values of these extremely thin regions are similar enough to the surrounding soft tissues that they 'disappear' when the soft tissues are digitally rendered transparent.

The text and figures from this paper are complemented by the following 3-D reconstructions animated to rotate around the x and y axes: adult (FMNH 215541) and juvenile (TNHC 62987) braincases (Appendices 1 and 2), skull and associated osteoderms of the adult (FMNH 215541) (Appendix 3), and the digital endocast of the left inner ear cavities of the adult (FMNH 215541) (Appendix 4). Slice-by-slice animations along the coronal axis also are provided for both the adult (FMNH 215541) and juvenile specimens (TNHC 62987) (Appendices 5 and 6).

Additional digital animations of skulls and skull elements for both the adult and juvenile specimens were scanned and posted at http://www.digimorph.org/specimens/Shinisaurus_crocodylus/

adult and http://www.digimorph.org/specimens/Shinisaurus_crocodylus/juvenile. These images include 3D reconstructions (animated to rotate around the three orthogonal axes) of the entire skull, articulated braincase, isolated orbitosphenoids, isolated sphenoid, isolated basioccipital, isolated supraoccipital, isolated prootic, isolated otooccipital, and isolated stapes. Additional imagery for the juvenile includes slice-by-slice animations along the three orthogonal axes, 3-D cutaway animations along the three orthogonal axes, and an inspeCTor Java viewer applet. Additional animations for the adult specimen include 3-D digital endocast of the left inner ear cavities rotating around the three orthogonal axes, and 3-D reconstructions of the skull with osteoderms digitally removed rotating around the three orthogonal axes.

In addition to the CT data sets, we referred to two dry skeletal preparations of *S. crocodylus*. A specimen from the University of California Museum of Vertebrate Zoology (MVZ 204291) includes an articulated skull of an adult of unspecified SVL. A juvenile specimen from the Quaternary Sciences collection at Northern Arizona University (NAUQSP 17563) has a disarticulated skull and SVL of 59 mm.

Unless otherwise specified, terminology follows that used by S.E. Evans in a forthcoming paper to be published in Volume 20 of *Biology of the Reptilia*. Two exceptions are: 1) we do not use directional terms in the naming of processes and 2) we adopt a standard usage for the terms 'foramen' and 'fenestra'. We use 'foramen' for a penetration within a bone and 'fenestra' for openings between bones; a notable exception to this is our retained usage of the commonly accepted 'foramen magnum.'

DESCRIPTION

Braincase

General Features of the Braincase (Figure 1). The description of the individual braincase elements provided here is based primarily on the adult specimens. Some observations on the juveniles are also referenced in the description, but a summary of our observations on ontogenetic differences in braincase features is provided in the discussion. The ossified braincase of *S. crocodylus*, like most lizards, consists of an orbitotemporal region represented by the paired orbitosphenoids and an otooccipital region consisting of a midline anteroventral sphenoid (a composite element that includes the chondrocranial basisphenoid and dermatocranial parasphenoid), a midline posteroven-

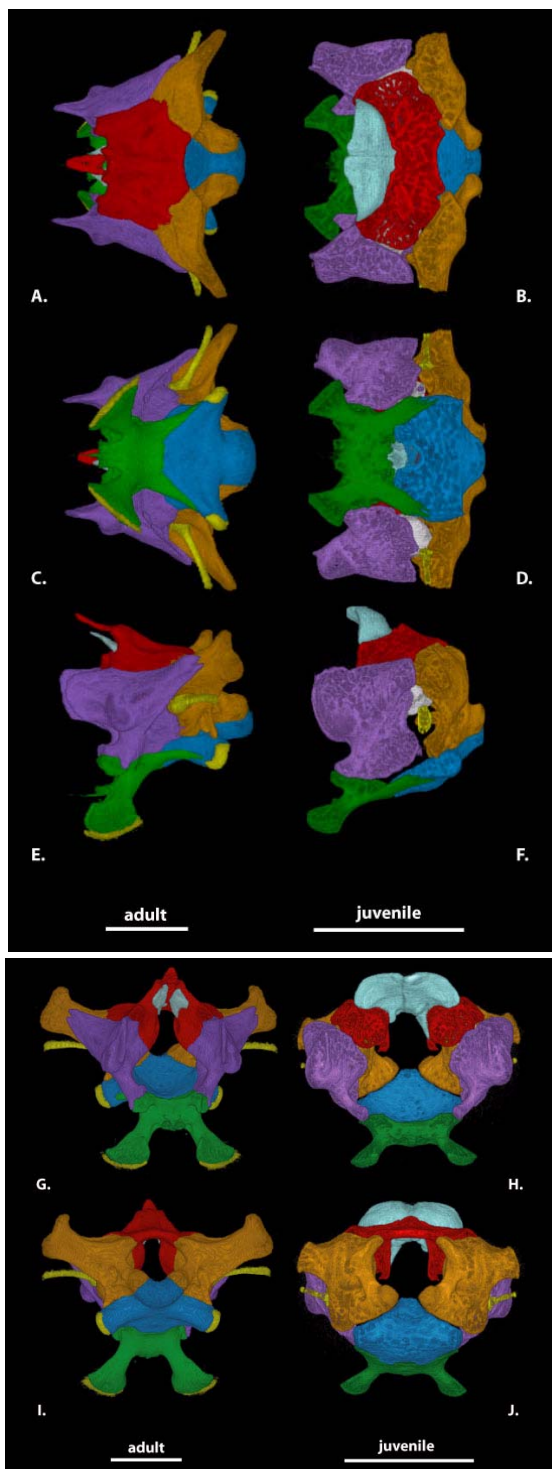


Figure 1. Digital renderings of the articulated braincase of adult (FMNH 215541) and juvenile (TNHC 62987) *Shinisaurus crocodilurus*. The adult specimen is depicted on the left (A, C, E, G, I), the juvenile on the right (B, D, F, H, J). A-B: dorsal view; C-D: ventral view; E-F: left lateral view; G-H: anterior view; I-J: posterior view. Green = sphenoid; dark blue = basioccipital; red = supraoccipital; purple = prootic; orange = otooccipital; pale blue = calcified endolymph; white = statolith mass. Anterior is to the left in A-F; dorsal is to the top in G-J. Scale bar = 5 mm.

Table 1. Braincase length and condylobasal skull length of two specimens of *Shinisaurus crocodilurus*. Braincase length was measured from the posterior margin of the occipital condyle to the anterior margin of the basisphenoid at midline (i.e., between the trabeculae cranii). No parasphenoid ossification was included in this measurement. BCL, length of braincase; CBL, condylobasal length.

Specimen	BCL (mm)	CBL (mm)	BCL/CBL as a percentage
FMNH 215511 (adult)	4.33	9.18	29
TNHC 629987 (juvenile)	15.43	31.25	28

tral basioccipital, a midline dorsal supraoccipital, paired anterior prootics, and paired posterior otooccipitals (opisthotic and exoccipital). The otooccipital elements fuse into a single unit in the adult (Zhang 1991). The fusion of the opisthotic and exoccipital occurs prenatally in most squamates (Estes et al. 1988; Maisano 2001) but are partially separated in some juvenile *S. crocodilurus*. The length of the braincase relative to the total length of the skull is similar in both the juvenile and adult specimens we scanned (Table 1).

The braincase as a unit articulates with the pterygoids via the basipterygoid processes of the sphenoid, the epipterygoids via the alar processes of the prootics, the parietals via the ascending process of the tectum synoticum (see Supraoccipital), the squamosals via the paraoccipital processes (see Otooccipital), and the vertebral column via the occipital condyle and the flexor and extensor musculature of the neck (Oelrich 1956).

Orbitosphenoid (Figure 2). Because of their relatively small size and lack of contact with other ossified elements, the orbitosphenoids are often lost or overlooked in standard skeletal preparations. The orbitosphenoids of *S. crocodilurus* were not studied or described by McDowell and Bogert (1954), Wu and Huang (1986), Zhang (1991), or Conrad (2004). The presence of orbitosphenoids in *Xenosaurus* is subject to variation, with bilateral asymmetry reported in some specimens (Evans, personal commun., 2004). CT data sets reveal their presence in *S. crocodilurus* and document that they are well developed even in the juvenile.

The paired orbitosphenoids, which ossify from the embryonic pila metoptica and form the orbitotemporal portion of the osseous braincase (Bellairs and Kamal 1981), lie anterior and medial to the epipterygoids in a position that approximates the posterior margin of the orbits. The orbitosphenoids consist of a pair of mediolaterally flattened, rod-like bones that are oriented anterodorsally-posteroven-

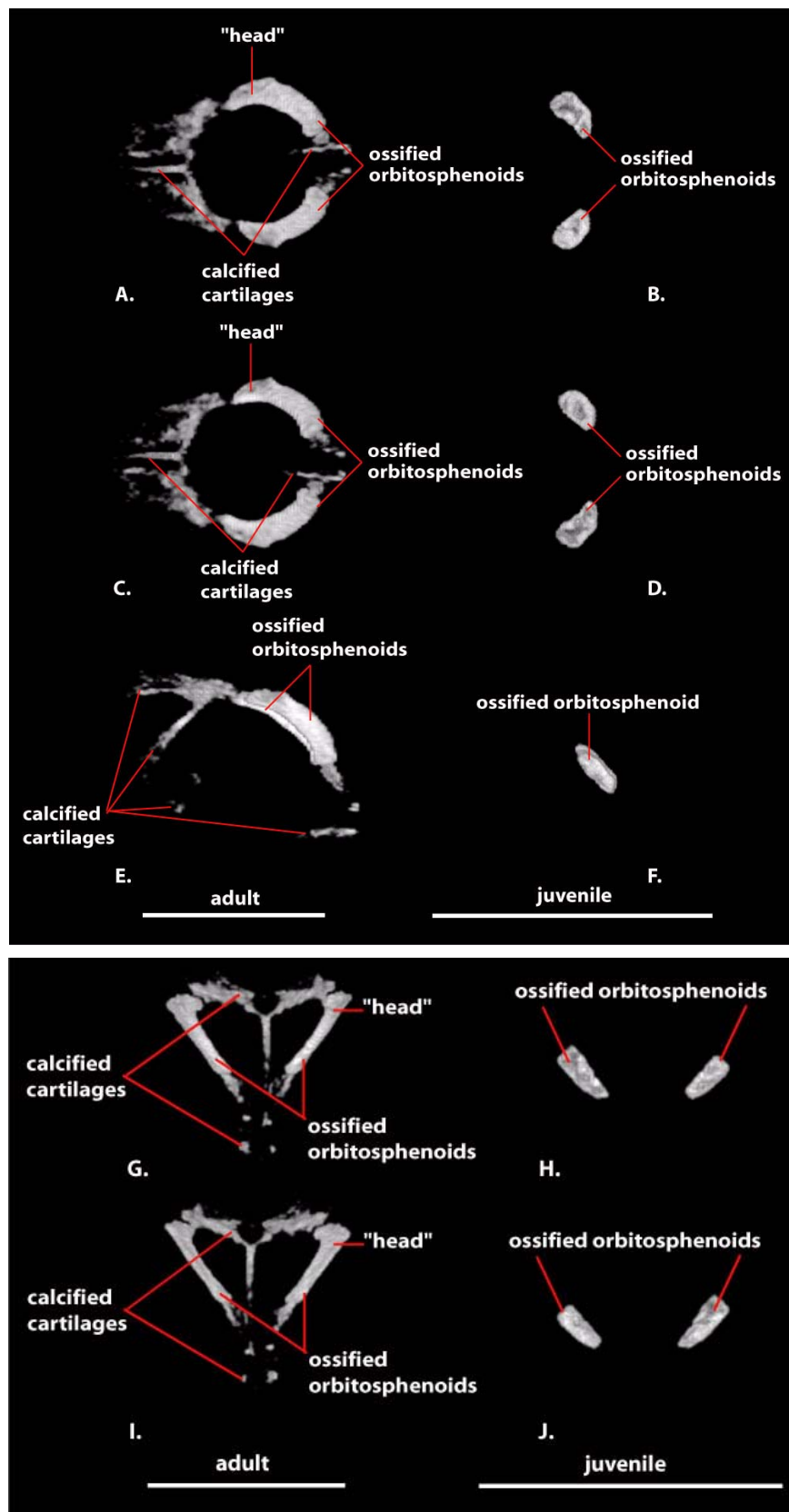


Figure 2. Digital reconstruction of the orbitosphenoid and surrounding calcified cartilages of *S. crocodilurus*. The adult specimen (FMNH 215541) is depicted on the left (A, C, E, G, I), the juvenile (TNHC 62987) on the right (B, D, F, H, J). A-B: dorsal view; C-D: ventral view; E-F: left lateral view; G-H: anterior view; I-J: posterior view. Anterior is to the left in A-F; dorsal is to the top in G-J. Scale bar = 5 mm.

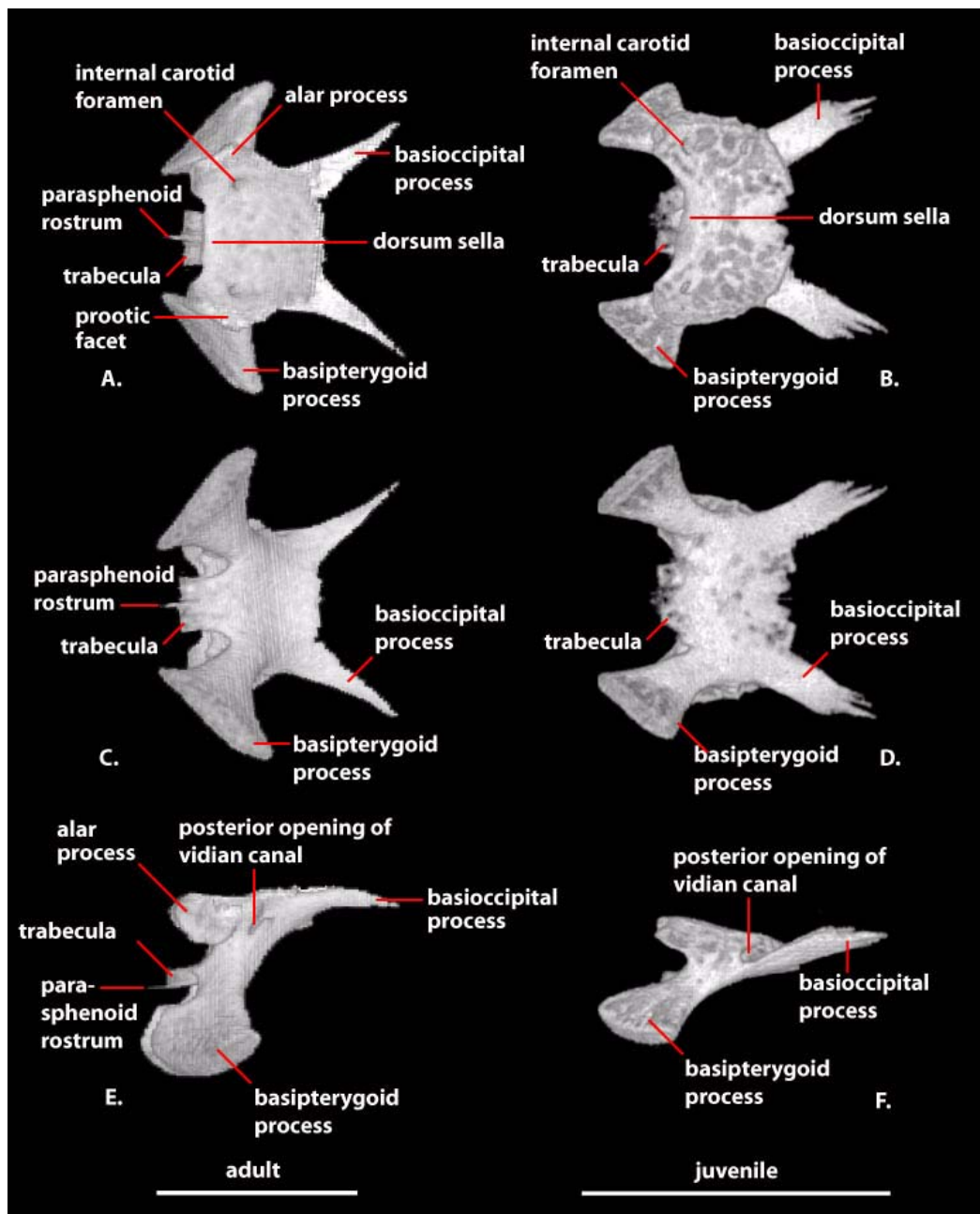


Figure 3. Digital reconstruction of the sphenoid of *S. crocodilurus*. The adult specimen (FMNH 215541) is depicted on the left (A, C, E, G, I), the juvenile (TNHC 62987) on the right (B, D, F, H, J). A-B: dorsal view; C-D: ventral view; E-F: left lateral view; G-H: anterior view; I-J: posterior view. Anterior is to the left in A-F; dorsal is to the top in G-J. Scale bar = 5 mm.

trally, but whose dorsal ends lie distinctly anterior and lateral to their ventral ends. A convex postero-dorsal margin, a concave anteroventral margin, and an anteroposteriorly expanded dorsal ‘head’ give these bones a costiform appearance when viewed as isolated elements (Figure 2A, C). They are approximately symmetrical in size and shape. Several of the calcified cartilages that support the

membranous braincase are visible in the CT data set of the adult specimen (FMNH 215541).

Sphenoid (Figure 3). The sphenoid is an irregularly shaped compound bone that is composed of the chondrocranial basisphenoid underlain and tightly fused to the dermatocranial parasphenoid. The sphenoid forms strong sutural contacts with the prootic anterodorsally and the basioccipital posteriorly. The suture with the basioccipital is

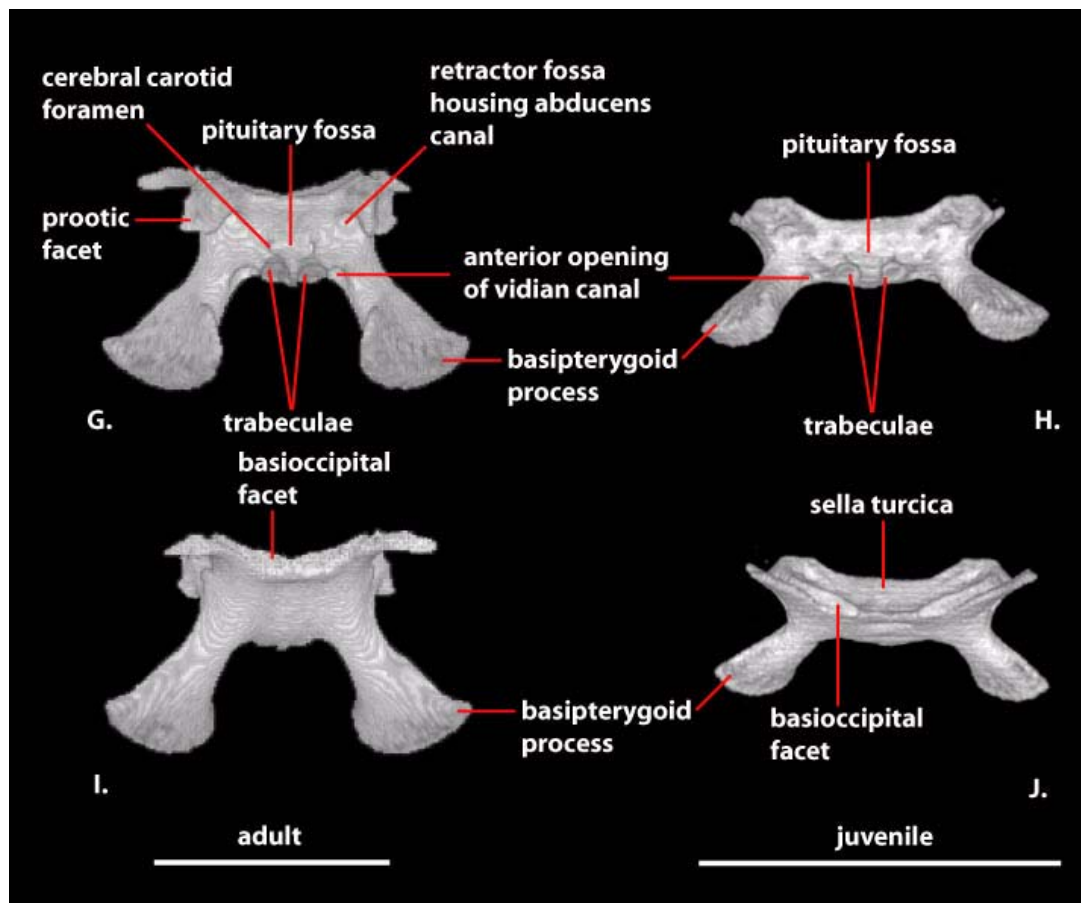


Figure 3 (continued).

transversely oriented medially and extends posterolaterally along a pair of elongated basioccipital processes ('triangular arms' of McDowell and Bogert 1954) of the sphenoid that run along the lateral margin of the basioccipital and contribute to the anterior margins of the basal tubera ('muscular tuberosity' of McDowell and Bogert 1954; 'sphenoccipital tubercles' of Oelrich 1956). This contribu-

tion to the basal tubera was considered a synapomorphy of *Xenosaurus* + *S. crocodilurus* by Rieppel (1980). These processes account for nearly one-half of the total length of the sphenoid and reach a point that is nearly level with the posterior margin of the fenestra ovalis (McDowell and Bogert 1954). The distal ends of the basioccipital processes of NAUQSP 17563 and TNHC 629987 have secondary, fingerlike processes (Figure 4) that are absent in FMNH 215541 and asymmetrically reduced (right) or lost (left) in MVZ 204291.

A distinct unossified area at the sphenoid-basioccipital suture (basicranial fontanelle) was noted by McDowell and Bogert (1954) on AMNH 44928 (Rieppel 1980, figure 20). It is absent in FMNH 215541 and MVZ 204291, where the region is fully ossified and only a shallow dimple is present on the ventral side of the suture. A large and distinct basicranial fontanelle is present along the sphenoid-basioccipital suture in TNHC 62987 (Figure 5). When the disarticulated sphenoid and basioccipital of NAUQSP 17563 are articulated, the fontanelle also clearly is present; the disarticulated elements clearly preserve the margins (Figure 4). Based on figure 20 of Rieppel (1980) and its asso-

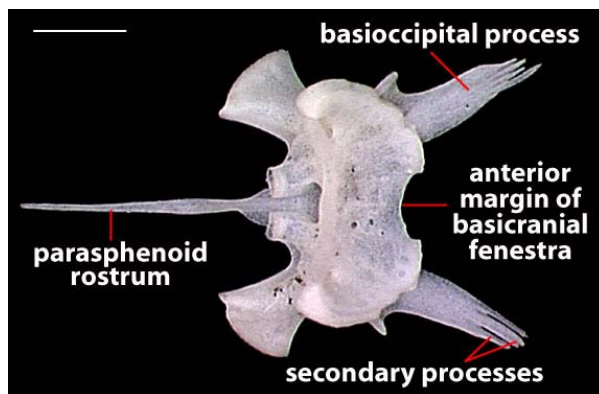


Figure 4. Dorsal view of the sphenoid of *S. crocodilurus* (NAU QSP 17563). Anterior is to the left. Scale bar = 1 mm.

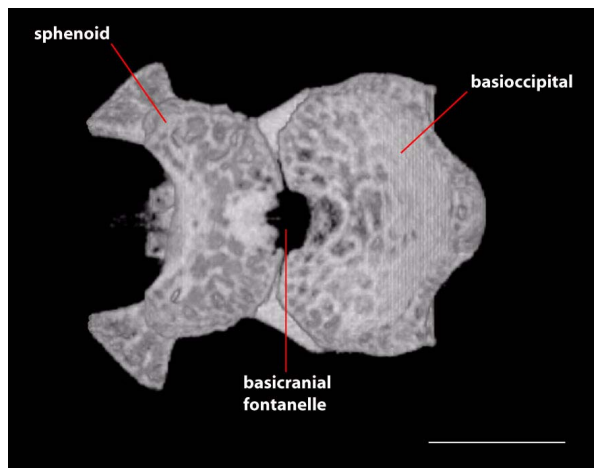


Figure 5. Digital reconstruction of the articulated sphenoid and basioccipital of juvenile *S. crocodilurus* (TNHC 62987) in ventral view. Anterior is to the left. Scale bar = 2 mm.

ciated scale bar, the condylobasal length of AMNH 44928 is between 22 and 23 mm, which is considerably shorter than the same measurement in FMNH 215541 (31.25 mm) and MVZ 204291 (32.7 mm). The fact that most authors who commented on the skull morphology of *S. crocodilurus* were utilizing skeletally immature specimens was noted by Conrad (2004). It is possible that absence of the fontanelle can be used to mark skeletally mature specimens; if so, skeletal maturity is reached between 23 mm and 32 mm.

Anteroventrally the sphenoid participates in the synovial palatobasal articulation with the pterygoids via the well-developed basipterygoid processes (McDowell and Bogert 1954). Pads of calcified cartilage cover the distal surface of the basipterygoid processes in the adult (Figure 6).

A distinct and well-ossified parasphenoid rostrum is present in NAUQSP 17563 (Figure 4). A distinct process also is discernible in the digital data set of FMNH 215541, but the bone was thin enough that the CT renderings show gaps in part of the rostrum (Figure 7). A well-developed rostrum was also depicted by Zhang (1991, figures 5, 6). No distinct parasphenoid rostrum is preserved on MVZ 204291; instead a short, forked rostrum is present, with each arm of the fork situated beneath the medial side of the trabeculae (Figure 8). A short, unforked rostrum that extends beyond the anterior margin of the basipterygoid processes was illustrated by Conrad (2004, figure 14B). The range of variation in expression of the parasphenoid rostrum in *S. crocodilurus* is unknown.

Paired vidian canals extend through the sphenoid, their margins formed by the basisphenoid (above) and parasphenoid (below; Bellairs and

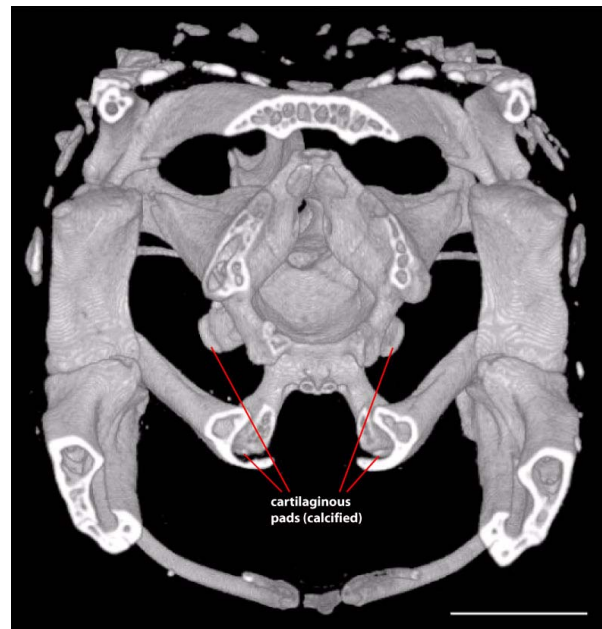


Figure 6. Coronal cutaway slice of adult *S. crocodilurus* (FMNH 215541) illustrating calcified cartilaginous pads on the distal ends of the basipterygoid processes of the sphenoid and the basal tubers of the basioccipital. Scale bar = 5 mm.

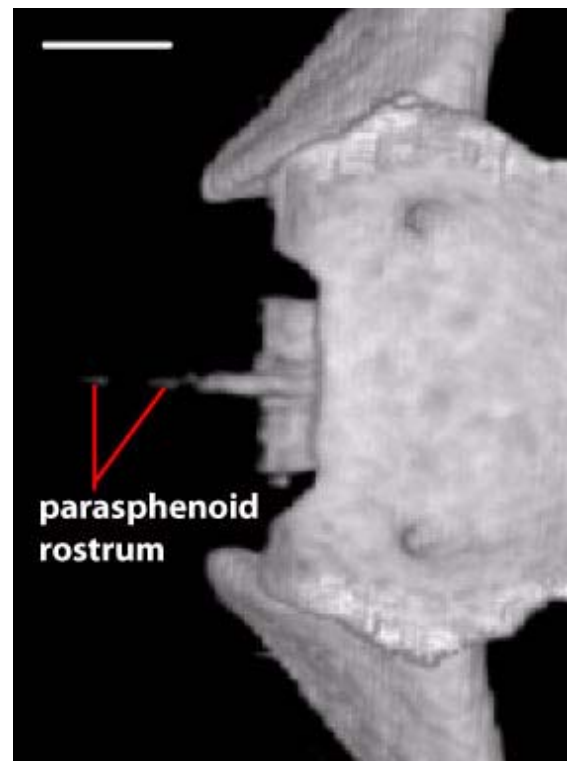


Figure 7. Dorsal view of the anterior portion of the sphenoid of adult *S. crocodilurus* (FMNH 215541) illustrating ossification of the parasphenoid rostrum. The separation of the ossifications is an artifact of the digital rendering process (see text for explanation). Anterior is to the left. Scale bar = 1 mm.

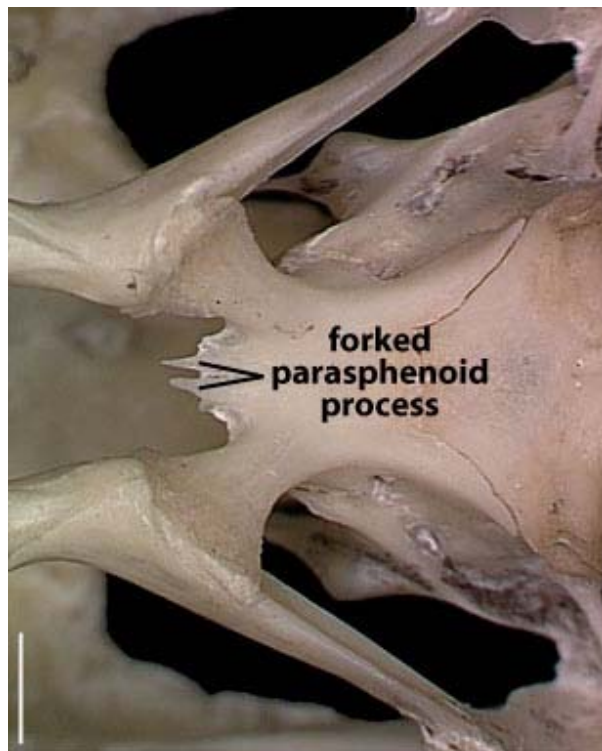


Figure 8. Ventral view of the sphenoid and surrounding region of adult *S. crocodilurus* (MVZ 204291) illustrating forked parasphenoid process. Anterior is to the left. Scale bar = 2 mm.

Kamal 1981). The anterior openings of these canals are positioned ventrolaterally and just posterior to the bases of the trabeculae cranii, and transmit the palatine artery and palatine branch of the facial nerve (cranial nerve VII). From its anterior opening, the vidian canal extends posterodorsally along a straight path that parallels and lies lateral to the trabecula. At a position just posterior to the trabecula, the vidian canal splits sending a short canal medially. This split is the osseous signature of the bifurcation of the internal carotid artery from which an anterior branch (palatine artery) and medial branch (cerebral carotid artery) are derived. The position of this split is close enough to the pituitary fossa that the 'canal' communicating the cerebral carotid artery to the floor of the fossa is extremely short. Behind this bifurcation, the vidian canal continues posterodorsally and slightly laterally before opening onto the lateral wall of the braincase.

The posterior opening of the vidian canal lies fully within the sphenoid, and is positioned a short distance below and behind the suture of the alar process of the sphenoid with the anterior inferior process of the prootic. Our observations are consistent with those of Conrad (2004) for the position

of the posterior opening in the sphenoid, but the dorsal border of the posterior opening of the vidian canal was described as being formed by the prootic by McDowell and Bogert (1954). The fact that this was likely in error was noted by Underwood (1957), but *S. crocodilurus* was scored as having the posterior opening of the vidian canal on the sphenoid-prootic suture by Estes et al. (1988, p. 223; see comment associated with synapomorphy 1 under Anguinae). That scoring may be based on the description provided by McDowell and Bogert (1954); alternatively, the position of this opening is polymorphic for *S. crocodilurus*. These conflicting observations also may be due to the complex configuration of the articulated skull in this region. The posterior opening of the vidian canal is immediately dorsal to the posterior basioccipital process of the sphenoid. This process obscures the sutural contacts of the basioccipital, prootic, and sphenoid, and in the articulated skull the dorsal border of the posterior vidian canal may appear superficially to be formed by the prootic (Conrad 2004). The posterior opening of the vidian canal was reported to be subject to individual variation across ontogenetic stages in some lacertid lizards by Barahona and Barbadillo (1998).

The recessus vena jugularis (Oelrich 1956) extends as a prominent canal groove from the posterior opening of the vidian canal posterodorsally and marks the path of the internal carotid artery, the lateral head vein, and the vidian branch of the facial nerve (Oelrich 1956). This groove extends only a short distance in the sphenoid with most of its length occurring in the prootic beneath the crista prootica (see Prootic).

The sella turcica, which houses the hypophysis of the pituitary body, is deep but obscured in dorsal view by the well-developed and widely overhanging dorsum sella. This overhang is especially prominent laterally where distinct clinoid processes are drawn anteriorly. At their greatest dorsal extent, the clinoid processes of the sphenoid fail to contribute to the incisura prootica, the osseous margin of which is formed completely by the prootic. A large canal housing the abducens nerve (VI) penetrates each side of the dorsum sella along a straight, posterodorsal path. These canals are positioned laterally with their anterior openings emerging beneath the clinoid processes into rather deep lateral pockets. These lateral pockets are more deeply invaginated than those in most other lizards (e.g., *Chamaeleo*, *Stellio*, *Acanthasaura*, *Sauromalus*, *Iguana*, *Sceloporus*, *Eublepharis*, *Mabuya*, *Platysaurus*, *Gerrhosaurus*, *Tupinambis*, *Proctoporus*, *Elgaria*, *Anguis*, *Ophisaurus*, *Varanus*, and *Heloderma*), but are approximately equivalent to those

in an adult *Xenosaurus grandis* (MVZ 128947). Some specimens of *Cordylus* also approach this condition. Each pocket is separated from the pituitary fossa by the crista trabecularis, a posterior extension of the trabecula cranii.

In the floor of the pituitary fossa, directly posterior and medial to the trabeculae of the basisphenoid, is a pair of foramina that transmit the dorsal branch of the internal carotid artery (cerebral carotid artery). These foramina are smaller than the anterior openings of the vidian canal and closely approximate the sagittal midline of the sella turcica. The position of carotid foramina within the sella turcica is variable in other anguimorphs (e.g., *Varanus*; Rieppel and Zaher 2000).

The sella turcica narrows anteriorly where the sphenoid forms a short rostrum. The basisphenoid contribution to this rostrum (ossified trabeculae communis-tropibasic skull) is easily discernible from the underlying parasphenoid, which extends further anteriorly.

Basioccipital (Figure 9). The basioccipital ossifies within the posterior portion of the embryonic basal plate and forms the posterior floor of the ossified braincase. The basioccipital contacts the otooccipitals dorsally, the sphenoid anteriorly and anterolaterally, and the prootics anterodorsally. In juvenile specimens, the posterior margin of the large basicranial fontanelle is formed by the basioccipital (Figure 5). Two prominent basal tubera extend from the posterolateral margin. These tubercles receive the insertion of the *longus capitis* muscles (Rieppel and Zaher 2000). The CT data set of the adult clearly reveals the presence of calcified cartilages on the distal surfaces of the basal tubera (Figure 6), but these are not visible in the juvenile.

The basioccipital does not contribute to the floor or the medial aperture of the recessus scala tympani. It forms the ventral margin of the foramen magnum and the middle portion of the occipital condyle. The occipital condyle is concave dorsally in posterior view (Conrad 2004). The dorsal surface of the basioccipital houses a shallow depression just anterior to the basal tubercle. That depression is confluent with a triangular space formed between the crista interfenestralis and the crista tuberalis in the otooccipital that terminates at the lateral aperture of the recessus scala tympani (see Otooccipital). Near the junction of the basioccipital, otooccipital, and prootic the dorsal surface of the basioccipital shows another shallow depression that marks the bottom of the lagenar recess, the ventral terminus of the cavum cochleare (Wever 1978).

Supraoccipital (Figure 10). The supraoccipital forms the roof of the ossified braincase and the dorsal margin of the foramen magnum. It contacts the otooccipital posteroventrally and the prootic anteroventrally. The ossified base of the ascending process of the tectum synoticum is present and contacts the parietal (McDowell and Bogert 1954). The ascending process is heavily calcified in the adult but lacks a solid contact with the main body of the supraoccipital (Figure 10A). A weakly developed sagittal crest extends along the dorsal midline (McDowell and Bogert 1954), declining in prominence posteriorly. The supraoccipital forms the top of the otic chamber, housing the canals for the anterior and posterior semicircular ducts as well as the osseous common crus where the two canals join within the otic capsule (see Inner Ear).

The opening for the endolymphatic duct as it passes from the otic chamber is exposed in medial view and lies completely within the supraoccipital. At its posterior edge, the margin of the foramen is not sharply defined, but rather is formed by the angled slope of the posterior portion of the tympanic bulla. The foramen appears to be partially divided in FMNH 215541 (Figure 11). The overall appearance is of a canal oriented anteroventrally to posterodorsally. Calcified endolymph is present in both scanned specimens and appears in the CT data sets as bright white masses lying along the ventral margin of the supraoccipital. In our colored renderings of the braincase the endolymph appears in pale blue (Figure 1G, H). In the adult (FMNH 215541) the endolymph appears as approximately symmetrical, small masses on either side of the bone. In the juvenile (TNHC 62987) the endolymph forms an extensive and somewhat asymmetrical mass that extends anteriorly approximately one-fifth of the way along the total length of the parietal.

Prootic (Figure 12). The prootic is a triradiate bone that ossifies in the anterior half of the otic capsule and contributes the anterior half of the osseous otic chamber. The prootic contacts the epipterygoid anterodorsally, the sphenoid anteroventrally, the basioccipital posteroventrally, the otooccipital posteriorly, and the supraoccipital dorsally. It does not contact the parietal or the quadrate in any of the specimens available to us, but was noted to do so by Conrad (2004) and Zhang (1991). In both cases, the prootic closely approaches these bones, but the CT data reveal no contact. A pair of elongate, anteriorly directed, mediolaterally compressed dorsal alar processes ('dorsal anterior wing' of McDowell and Bogert 1954) form the anteriormost extent of the osseous neurocranium. Elongate, anterodorsally directed alar processes of the

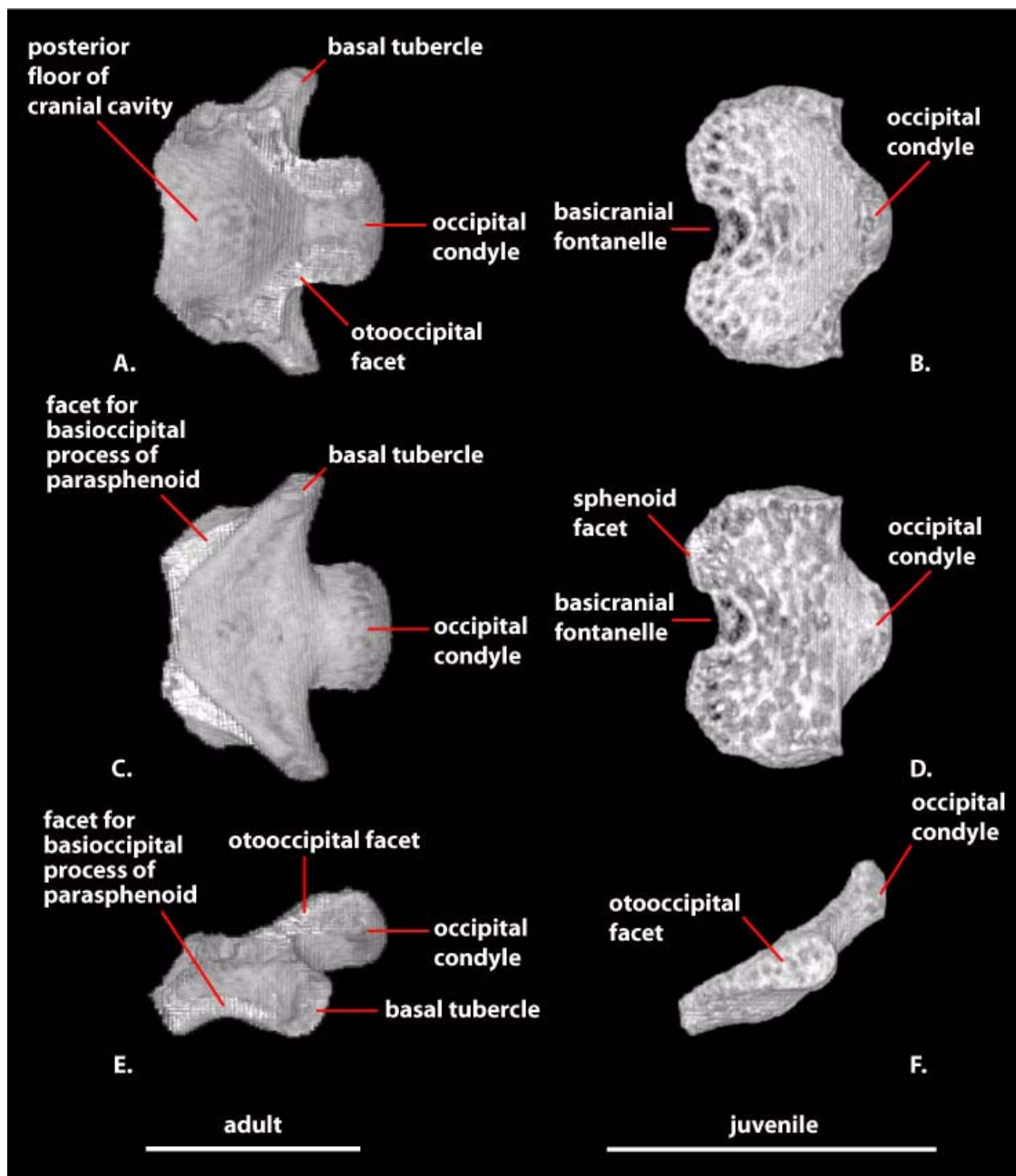


Figure 9. Digital reconstruction of the basioccipital of *S. crocodilurus*. The adult specimen (FMNH 215541) is depicted on the left (A, C, E, G, I), the juvenile (TNHC 62987) on the right (B, D, F, H, J). A-B: dorsal view; C-D: ventral view; E-F: left lateral view; G-H: anterior view; I-J: posterior view. Anterior is to the left in A-F; dorsal is to the top in G-J. Scale bar = 5 mm.

prootic were considered a synapomorphy of *Scleroglossa* by Estes et al. (1988). The alar process of the prootic contacts the dorsal tip of the epipterygoid and forms the dorsal margin of a prominent incisura prootica ('trigeminal notch' of McDowell and Bogert 1954) with contribution from the anterior ampullar recess (McDowell and Bogert 1954). The anterior ampullar recess extends far enough ventrally so that it appears to partially divide the incisura prootica in lateral view in some

specimens. The anterior inferior process of the prootic forms the ventral margin of the incisura prootica and contacts the dorsal margin of the sphenoid, but the sphenoid does not participate in formation of the incisura prootica.

The path of the anterior semicircular canal is visible as a prominent ridge on the lateral surface of the prootic in front of the crista prootica and just behind the alar process. The bone is extremely thin along the path of this canal, and in the 3-D digital

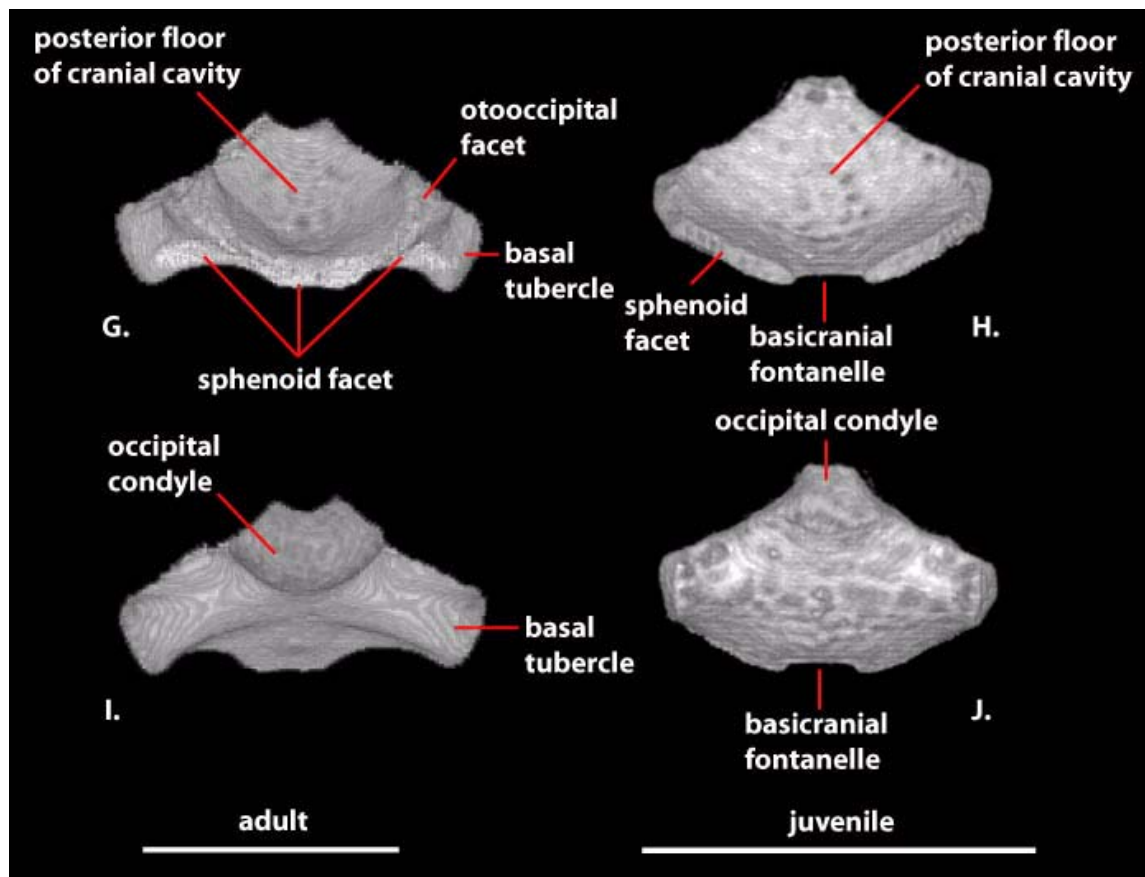


Figure 9 (continued).

renderings of the juvenile CT dataset the thinnest areas appear as holes in the bone; this is an artifact of the digital rendering process (see Methods).

The crista prootica is present as a prominent crest on the lateral surface of the prootic that extends posterodorsally from a point above the clinoid processes of the sphenoid to a point above the fenestra ovalis. This lamina of membrane bone (sensu Rieppel 1993) is not as well developed in *S. crocodilurus* (or *Xenosaurus*) as it is in *Varanus* (McDowell and Bogert 1954; Gauthier 1982), in which it partially obscures the fenestra ovalis when viewed laterally (Rieppel and Zaher 2000). In both *Xenosaurus grandis* and *S. crocodilurus*, the crest is most extensive (somewhat more so in *Xenosaurus*) at its posterodorsal end and is reduced in extent anteroventrally. A slight raised area along the clinoid process of the sphenoid near the suture with the prootic is continuous with the crista prootica in some specimens. The recessus vena jugularis is formed ventral to this crest and extends from the posterior opening of the vidian canal (in the sphenoid) to the anterior margin of the fenestra ovalis. It delineates the medial wall of the portion of the cranioquadrate space that transmits the lateral

head vein and the branches of the facial nerve. As a result of reduction in the crista prootica, this groove is not as well developed below the lateral facial foramen as it is above it.

The medial surface of the prootic contains the acoustic recess, a deep invagination that is penetrated by a single opening for the facial nerve (VII) and a pair of foramina for the acoustic (VIII) nerve. The facial foramen is ventrally located and much smaller than either the anterior or posterior acoustic foramina. The relative size of the auditory foramina exhibits considerable variation within and between anguimorph lizard species (Oelrich 1956; Norell and Gao 1997; Rieppel and Zaher 2000). The canal housing the facial nerve extends ventrolaterally through the prootic and exits into the cranioquadrate space via a single foramen. This lateral opening is positioned within the recessus vena jugularis anteroventral to the fenestra ovalis, slightly less than halfway between the fenestra ovalis and the prootic-sphenoid suture.

The lateral opening for the facial nerve was reported to be bifurcated in some anguimorph squamates (some *Varanus*, some mosasaurs; Rieppel and Zaher 2000) by a strut of bone that

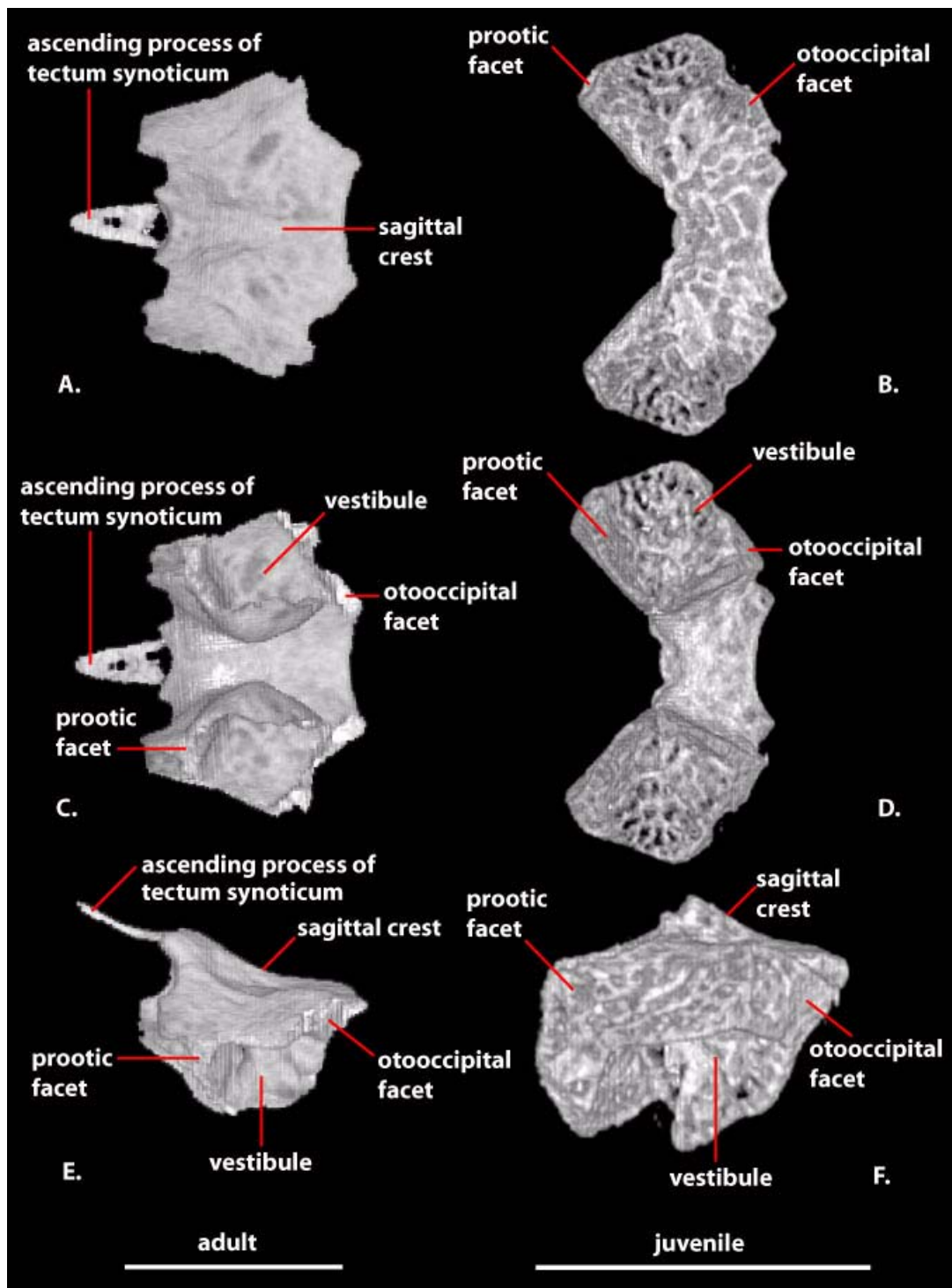


Figure 10. Digital reconstruction of the supraoccipital of *S. crocodilurus*. The adult specimen (FMNH 215541) is depicted on the left (A, C, E, G, I), the juvenile (TNHC 62987) on the right (B, D, F, H, J). A-B: dorsal view; C-D: ventral view; E-F: left lateral view; G-H: anterior view; I-J: posterior view. Anterior is to the left in A-F; dorsal is to the top in G-J. Scale bar = 5 mm.

extends across the groove, thus delineating separate paths for the anterior palatine and posterior hyomandibular branches of the facial nerve. Although none of our specimens show such a bifur-

cation, its presence in some *S. crocodilurus* was reported by Conrad (2004) who noted the potential importance of documenting variation in this feature. In MVZ 204291 a small extension of the crista

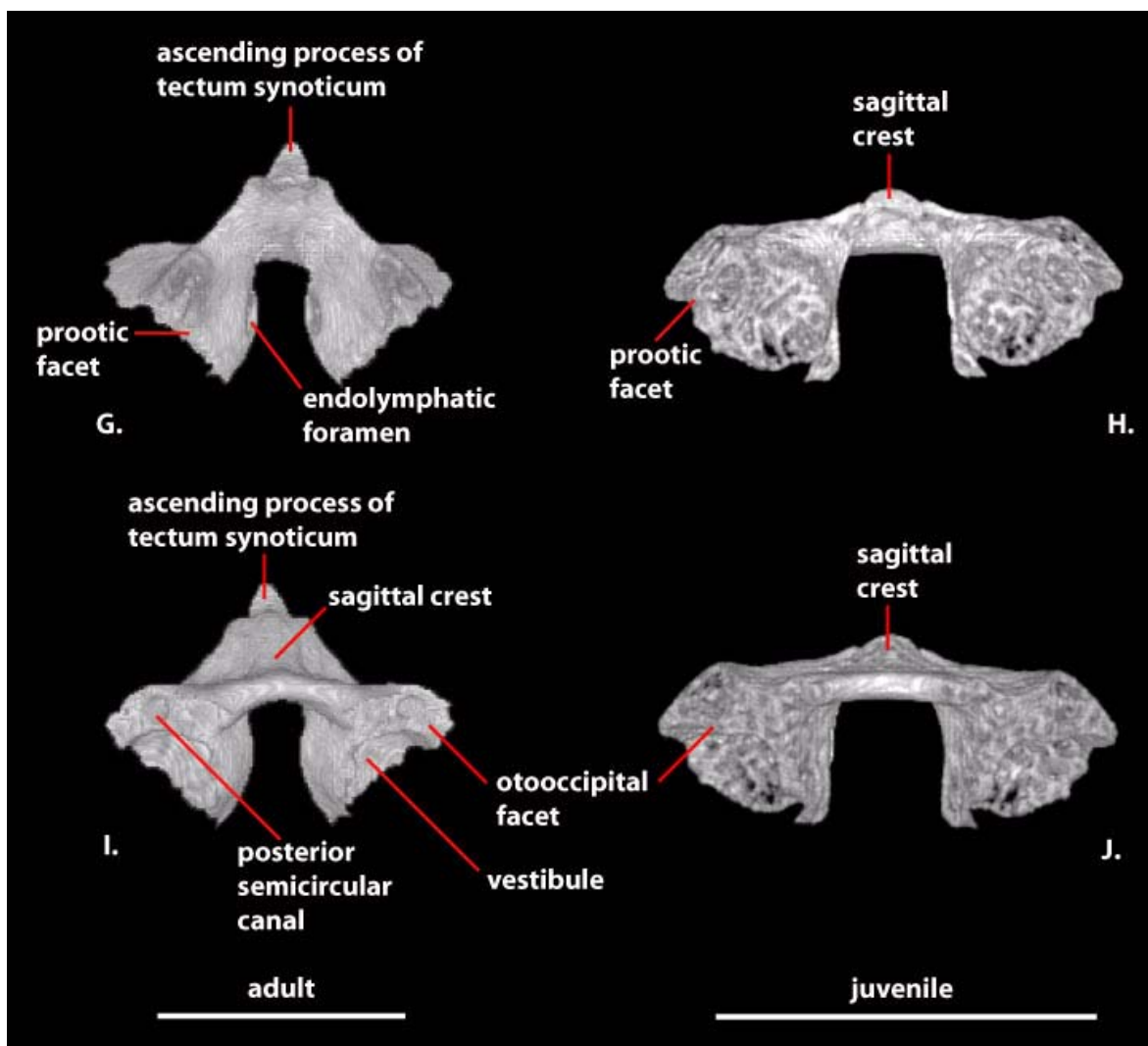


Figure 10 (continued).

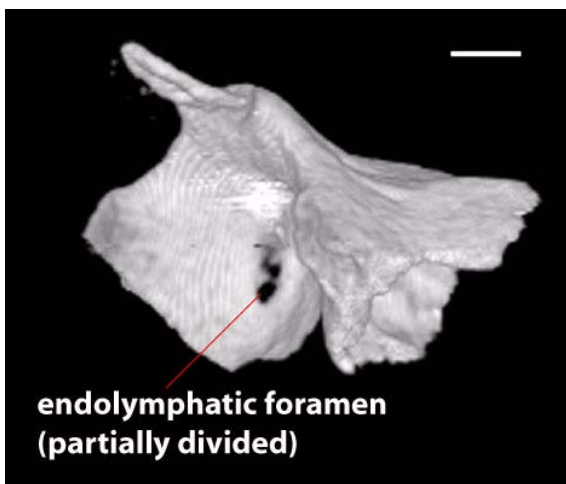


Figure 11. Oblique left lateral view of a digital reconstruction of the supraoccipital of an adult *S. crocodilurus* (FMNH 215541), showing partial division of the endolymphatic foramen. Scale bar = 1 mm.

prootica extends ventrally towards a bony upgrowth on the lateral wall of the prootic just anterior to the fenestra ovalis (Figure 13). This helps explain the presence of a bifurcation in some specimens, but regarding the resultant morphology as a bifurcation of the foramen is somewhat misleading. We examined two specimens of *Varanus exanthematicus* (California Academy of Sciences [CAS] 228520 and CAS 228521) and in both the facial nerve exits the braincase via a normal, single foramen. The appearance of a 'bifurcation' in the adult is a result only of the meeting of a ventral down-growth of the crista prootica with a dorsally directed flange of bone from the lateral wall of the prootic, clearly visible in the younger specimen (CAS 228521). The eventual fusion of the two flanges of bone creates a canal, positioned lateral to the facial foramen proper. It is through this canal that the two branches of the facial nerve pass. This is

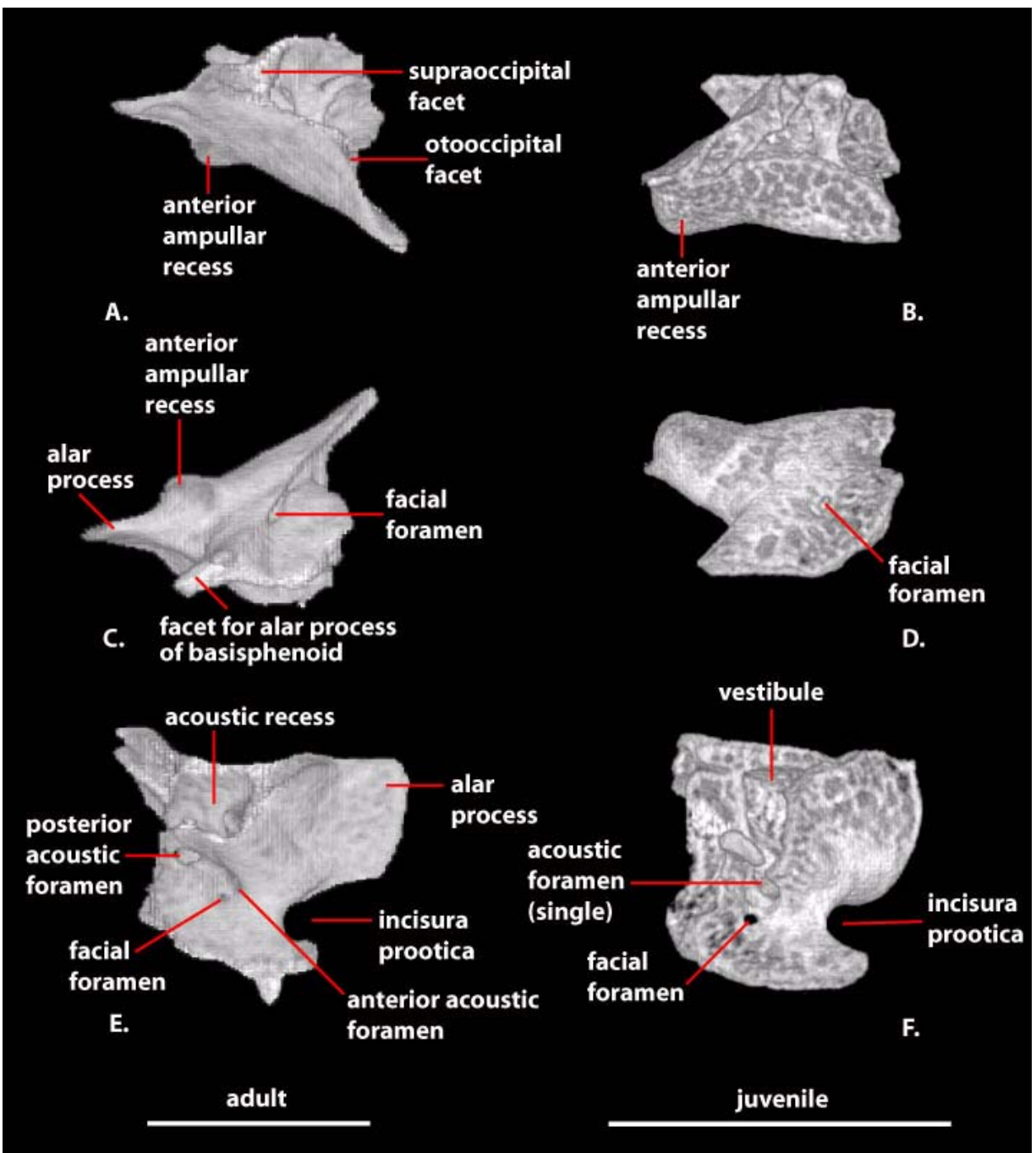


Figure 12. Digital reconstruction of the left prootic of *S. crocodilurus*. The adult specimen (FMNH 215541) is depicted on the left (A, C, E, G, I, K), the juvenile (TNHC 62987) on the right (B, D, F, H, J, L). A-B: dorsal view; C-D: ventral view; E-F: medial view; G-H: lateral view; I-J: anterior view; K-L: posterior view. Anterior is to the left in A-D and G-H; anterior is to right in E-F; dorsal is to the top in I-L. Scale bar = 5 mm.

similar to the development of an alisphenoid canal (or alar canal) in some carnivoran mammals in which a strut of bone obscures the foramen rotundum in lateral view (e.g., *Canis*; Evans 1993).

The acoustic foramina are situated within the acoustic recess and are positioned dorsal to the facial foramen. The anterior acoustic foramen is single, not paired as described in *Ctenosaura pec-*

tinata (Oelrich 1956). It lies above and slightly anterior to the facial foramen, whereas the posterior acoustic foramen lies distinctly behind and dorsal to both the facial and anterior acoustic foramen. The anterior acoustic foramen is slightly smaller than the posterior acoustic foramen, but both are distinctly larger than the facial foramen. The posterior foramen opens directly into the vestibule of the

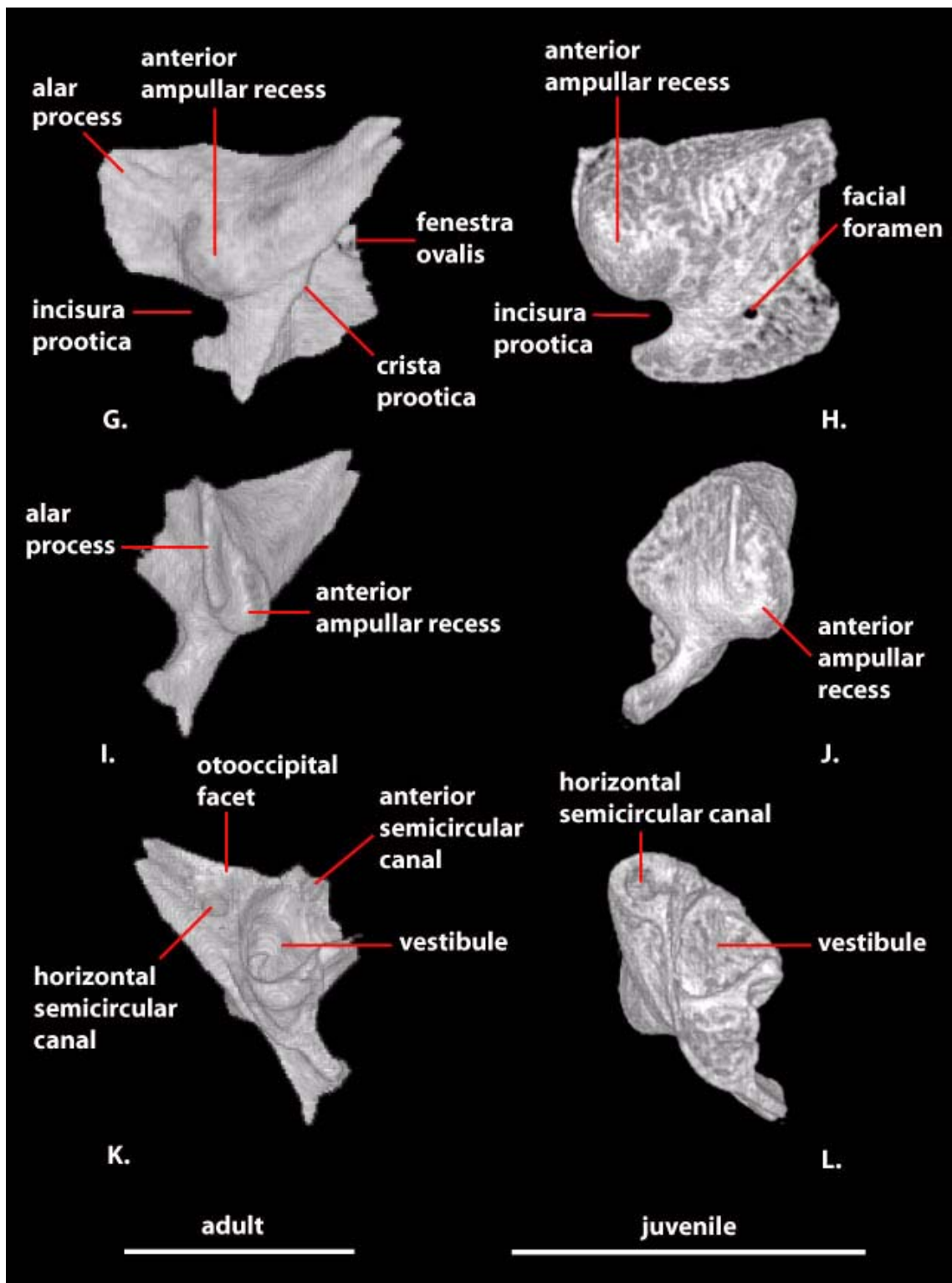


Figure 12 (continued).

cavum capsularis of the inner ear. The anterior foramen pierces the ventromedial wall of the anterior ampullar recess and transmits vestibular branches of the vestibulocochlear nerve (VIII) to the semicircular canals.

The fenestra ovalis ('foramen ovale' of Oelrich 1956; 'fenestra vestibuli' of Jollie 1960) is a subelliptical opening whose anterior margin is formed by the prootic and posterior margin by the otooccipital. It is distinctly asymmetrical in *S. crocodilurus*, with more than half of its diameter enclosed by the

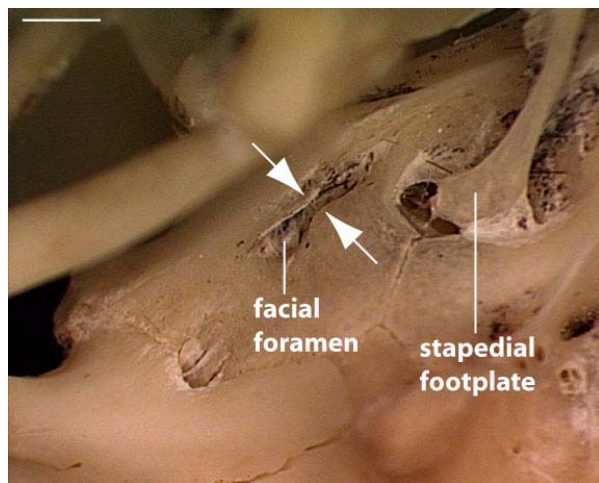


Figure 13. Lateral view of the braincase of an adult *S. crocodilurus* (MVX 204291). Note the close approximation of bone flanges forming a tunnel-like structure in the vicinity of the facial foramen. Anterior is to the left. Scale bar = 1 mm.

otooccipital. The fenestra ovalis is positioned above and anterior to the small lateral aperture of the recessus scala tympani. The fenestra also is anterior to the tip of the basal tubercle, which is in direct line ventral to the recessus scala tympani (in the plesiomorphic condition for Squamata the fenestra ovalis is in direct line dorsal to the tip of the basal tubercle [Norell and Gao 1997]; the relative shift in position of the fenestra ovalis in *S. crocodilurus* is shared with mosasaurs, but *Varanus* exhibits the plesiomorphic condition).

Ventral to the fenestra ovalis, the prootic and otooccipital are in contact again, forming, respectively, the anterior and posterior margins of the cavum cochleare. This cavity takes the form of an inverted pyramid, with the apex oriented ventrally. The ventral extremity (lagenar recess) houses the lagenae of the ear (Wever 1978).

The protractor pterygoidei, *pseudotemporalis profundus*, *pseudotemporalis superior*, and the 3c-layer of the *adductor mandibulae externus* all take their origin (at least in part) from the lateral surface of the prootic (Haas 1960; Rieppel 1980). The origin of the *protractor pterygoidei* lies largely along the lower margin of the incisura prootica and includes the inferior process of the prootic and the alar process of the sphenoid (some fibers continue along a tendon to take their origin on the postero-dorsal edge of the basiptyergoid process; Rieppel 1980). The *pseudotemporalis profundus* originates largely from the epiptyergoid with a posterior continuation of fibers onto the ventral edge of the alar process of the prootic (Haas 1960; Rieppel 1980). The *m. pseudotemporalis superficialis* (generally

given as *m. pseudotemporalis superior* by Haas [1960], but see p. 29 of his paper) also originates from the alar process of the prootic, although from a more dorsal position just behind the contact surface for the epiptyergoid, as well as from the ligamentous attachment of the alar process of the prootic to the descending process of the parietal (Rieppel 1980). The positioning in *S. crocodilurus* of the points of origin for the *m. pseudotemporalis superficialis* was considered to be derived by Rieppel (1980). The 3c-layer of the *m. adductor mandibulae externus* takes its origin on the alar process and crista prootica (Rieppel 1980).

Otooccipital (Figure 14). The otooccipital is formed from a fusion between the opisthotic and exoccipital. This fusion generally occurs during prenatal ontogeny and is considered a synapomorphy of Squamata (Estes et al. 1988; Maisano 2001). The original separation of the two elements is marked by the position of the vagus foramen (Figure 15; Conrad [2004:421] erroneously stated that the vagus foramen lies at the suture of the supraoccipital and the otooccipital, but his figure 15C accurately depicts and labels the vagus foramen). The bones are already fused in one juvenile specimen (TNHC 629987), but in NAUQSP 17563 the separation of the two elements is distinct ventrally (as it is in some hatchling lacertids and xantusiids; Rieppel 1992; Maisano 2001, 2002; Figure 15). The otooccipital is sutured to the prootic anteriorly, the supraoccipital dorsally, and the basioccipital ventromedially. Posterolaterally it contacts (via connective tissues) the quadrate, supraoccipital, and the postparietal process of the parietal. It does not contact the squamosal. The otooccipitals contribute the lateral and dorsolateral portions of the occipital condyle, form the lateral margins of the foramen magnum, and contribute substantially to the posterior braincase via strongly developed lateral extensions, the paraoccipital processes. The otooccipital forms more than half of the diameter of the fenestra ovalis.

Anteriorly the otooccipital contacts the prootic above and below the fenestra ovalis. The dorsal articulation facet between the two bones is pierced by the opening of the horizontal semicircular canal. The ventral articulation between the two bones is less expansive and forms the margin of the lagenar recess. On the lateral surface of the otooccipital just posterior and posteroventral to the fenestra ovalis is a broad, low ridge of bone, the crista interfenestralis (Säve-Söderbergh 1947). Its expression is reduced anteroventrally and does not extend as far as the prootic-otooccipital suture. Posterodorsally it merges with a sharply defined crest, the crista tuberalis (Säve-Söderbergh 1947) that runs

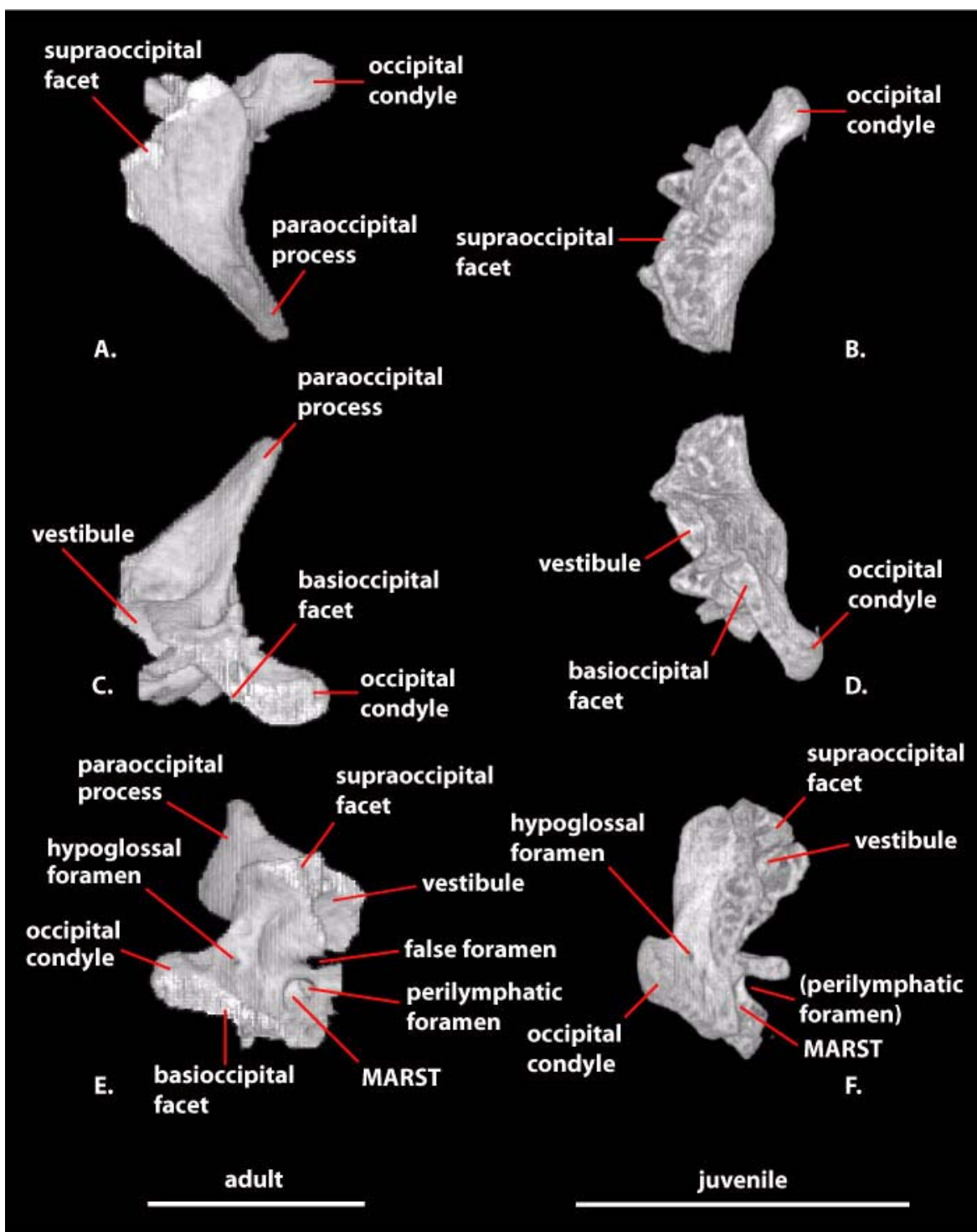


Figure 14. Digital reconstruction of the left otooccipital of *S. crocodilurus*. The adult specimen (FMNH 215541) is depicted on the left (A, C, E, G, I, K), the juvenile (TNHC 62987) on the right (B, D, F, H, J, L). A-B: dorsal view; C-D: ventral view; E-F: medial view; G-H: lateral view; I-J: anterior view; K-L: posterior view. Anterior is to the left in A-D and G-H; anterior is to right in E-F; dorsal is to the top in I-L. Scale bar = 5 mm.

approximately dorsoventrally from the ventral surface of the paraoccipital process to the dorsal margin of the basal tubercle. These two crests delimit a roughly triangular space near the dorsal apex of which is situated the small lateral aperture of the

recessus scala tympani (LARST; ‘foramen rotundum’ of Conrad 2004). Immediately posterior to the crista tuberalis the otooccipital is pierced by three foramina. The most dorsal of these is a crescent-shaped vagus foramen transmitting cranial nerve X

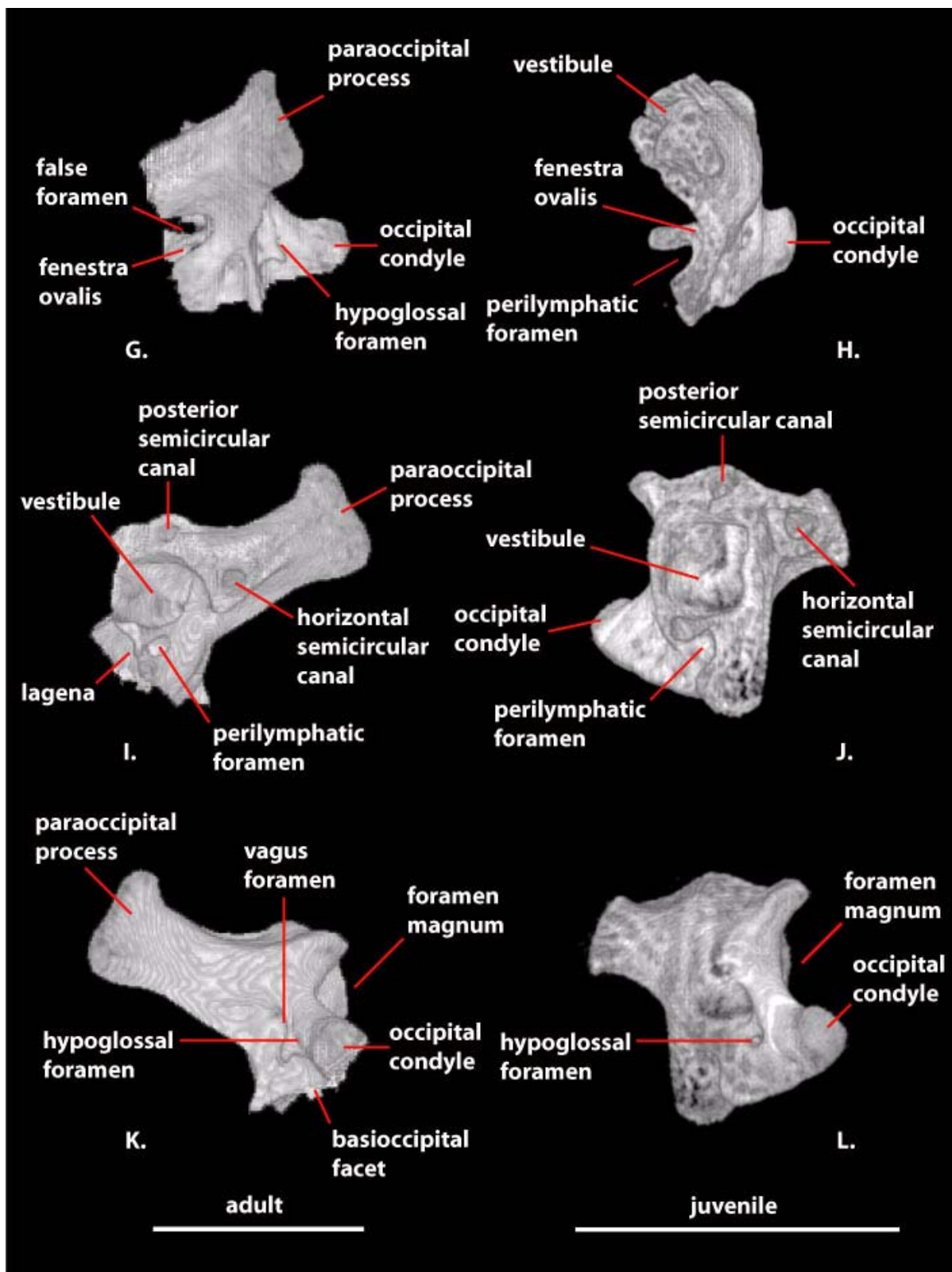


Figure 14 (continued).

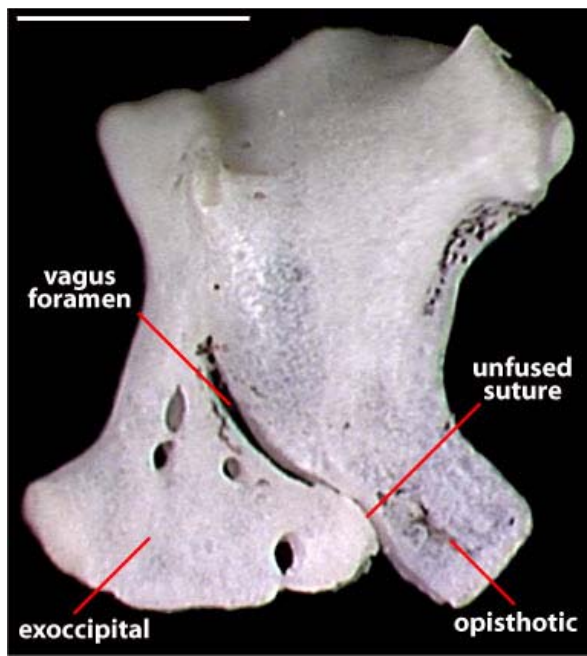


Figure 15. Posteroventral view of right otooccipital of juvenile *S. crocodilurus* (NAU QSP 17563). Complete fusion of the exoccipital and opisthotic has not yet occurred. Scale bar = 1 mm.

(according to Hu [1980] the accessory nerve [XI] merges with the vagus as soon as it leaves the brain). Ventral to this are two small hypoglossal foramina transmitting branches of cranial nerve XII. A third hypoglossal foramen is present posterior to these at approximately a level just ventral to the base of the vagus foramen.

The LARST is reduced in size relative to that of most other lizards. The medial extension of this space is similar to the normal condition for lizards, and a well-developed and fairly large medial aperture (MARST) is present. The recessus scala tympani appears to be contained entirely within the otooccipital in the CT data sets, although the basioccipital closely approaches the ventral margin. The MARST can be seen in an oblique posterolateral view looking through the foramen magnum. Just lateral to that opening, the perilymphatic foramen opens into the recessus from the vestibule. In the view through the foramen magnum (Figure 16), the two openings are essentially indistinguishable, a situation also found in other lizards (e.g., see caption to figure 11 in Bell et al. 2003:295). The perilymphatic foramen is positioned just ventral to an anteriorly projecting ledge of bone at the base of the vestibule that marks the recess for the ampulla of the posterior semicircular canal. Just dorsal to the vestibule, the articulation facet for the supraoccipital contains a penetration marking the passage of the posterior semicircular canal.

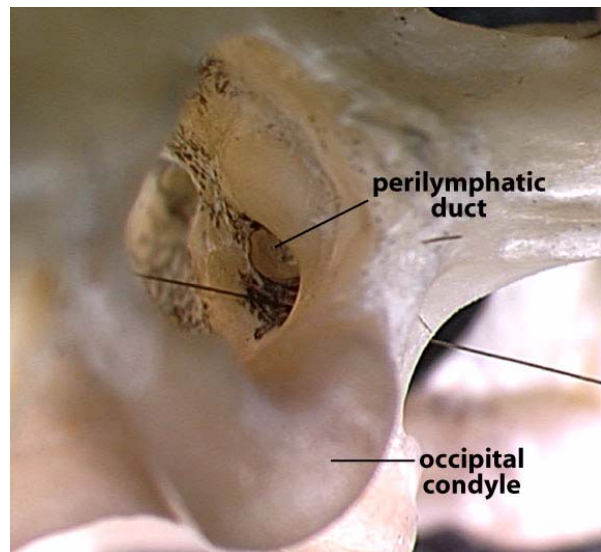


Figure 16. Posterolateral view of the right interior of the cranial cavity of adult *S. crocodilurus* (MVZ 204291). The view is through the foramen magnum toward the perilymphatic foramen and the medial aperture of the recessus scala tympani (RST). The long black hair passes through the lateral aperture of the RST (near the center of the right side of the image) and enters the cranial cavity via the medial aperture of the RST (near the center of the image). The width across the occipital condyle in this specimen is 3.9 mm.

In the CT data sets each vestibule is partly filled with a dense statolithic mass (Wever 1978) that appear as a bright white mass in the digital

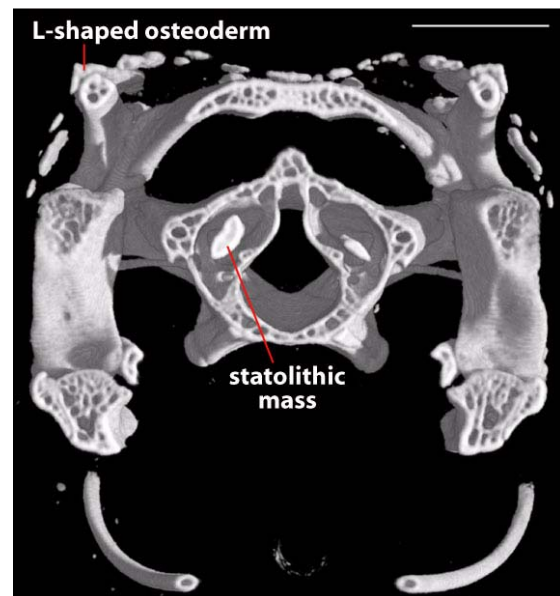


Figure 17. Coronal cutaway slice of adult *S. crocodilurus* (FMNH 215541) illustrating asymmetrical development of statolithic masses in the vestibule, and a cross-sectional view of an osteoderm clasping the canthal crest. Scale bar = 5 mm.

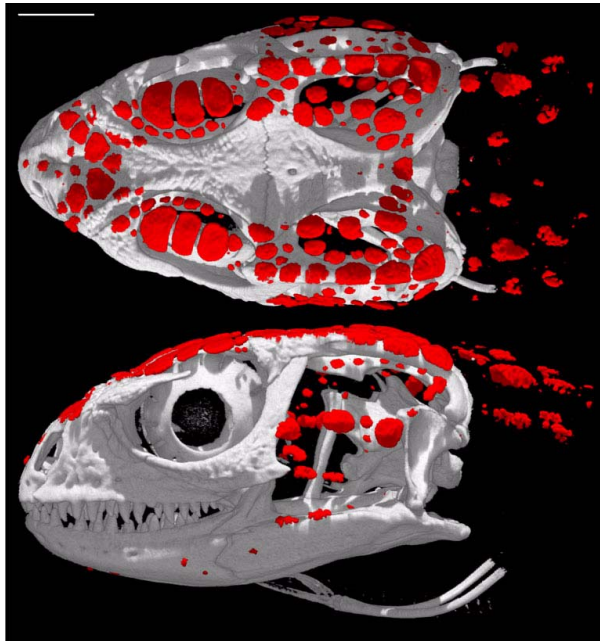


Figure 18. Digital reconstruction of the skull and associated osteoderms of an adult *S. crocodilurus* (FMNH 215541). Osteoderms are rendered in red. Top: dorsal view; bottom: left lateral view. Scale bar = 5 mm.

data sets. In the adult the statolithic mass is larger on the right side than on the left (Figure 17).

The paroccipital process forms the posterior portion of the lateral braincase and the ventral margin of the post-temporal fenestra. In the adult the lateral edge of the paroccipital process bears a dorsally oriented process with a slight medial inflection at its dorsal tip. This process contacts the supratemporal bone and the postparietal process of the parietal. At its lateral most edge, the paroccipital process contacts the cephalic condyle of the quadrate.

Cephalic Osteoderms

The presence of osteoderms in *S. crocodilurus* was noted previously by several authors (e.g., Borsuk-Bialynicka 1986; Wu and Huang 1986; Zhao et al. 1999; Hofmann 2000), but detailed discussion of their distribution and general morphology is lacking. The cephalic osteoderms in *S. crocodilurus* (Figure 18) do not contact each other and are not compound. They are not fused to the skull, and even in relatively large individuals they will pull free with the skin (the preserved skin of MVZ 204291 provides a clear view of the ventral surface of the cephalic osteoderms; Figure 19). They are concentrated along the dorsolateral margin of the head, with more limited distribution in the temporal region and neck and along the lower jaw. Osteoderms are mostly absent from the dorsome-

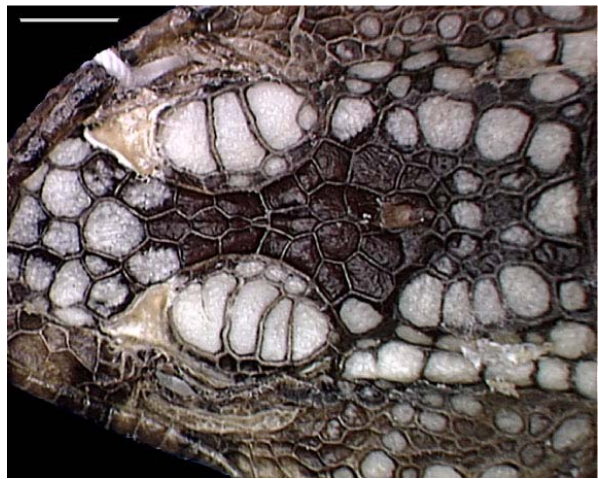


Figure 19. Ventral view of the cephalic skin of an adult *S. crocodilurus* (MVZ 204291) showing the osteoderms in place in the skin. Anterior is to the left. Scale bar = 5 mm.

dial and ventral aspects of the head. They are generally flat, plate-like structures with irregular margins and vary greatly in size, the largest being those that roof the orbit.

The osteoderms in the snout region exhibit a regular arrangement. Two small, subcircular osteoderms overlie the nasal process of the premaxilla at the midline and an array of larger osteoderms extend along each nasal/prefrontal and nasal/frontal contact onto the anterior end of the frontal; together these approximate a posteriorly pointing arrow. Two smaller osteoderms occur lateral and posterolateral to the tip of this arrow along each prefrontal/frontal contact.

Two linear series of osteoderms roof each orbit. The first runs just lateral to, and parallels the margin of, the frontal. It consists of eight small, subcircular osteoderms, the most anterior of which is the largest and overlies the palpebral, and the most posterior of which is the smallest and lies just anterior to the postorbitofrontal. The second series of osteoderms roofing the orbit parallels the first and consists of five osteoderms. The first and last are small and subcircular, whereas the middle three are plate-like and are the largest cephalic osteoderms.

Beginning where the postorbitofrontal clasps the frontoparietal suture, a field of mostly plate-like, moderately large osteoderms, extends posteriorly over the supratemporal fenestra and canthal crest, then medially to meet its opposite dorsal to the posterior margin of the parietal. This field can be broken down into three approximately linear series of osteoderms. The first series, consisting of roughly 12 osteoderms, lies along the lateral margin of the frontoparietal suture and parietal table. It

extends over the parietal near the base of the supratemporal process to meet its opposite, the bilaterally symmetrical series thereby forming the margins of a U-shaped osteoderm-free zone above the parietal. The second series, consisting of approximately seven osteoderms, lies entirely dorsal to the supratemporal fenestra and parallels the canthal crest. The third series, consisting of six osteoderms, actually clasps the canthal crest from its anterior margin to just anterior to the supratemporal. The latter series help to anchor an aponeurosis covering the upper temporal fenestra (Haas 1960). The posteriormost osteoderm in that series is the largest of the six, and these osteoderms are uniquely L-shaped in cross-section (Haas 1960:24; Figure 17).

In the temporal region ventral to the canthal crest is an array of osteoderms that is roughly E-shaped in left-lateral view. The dorsal arm of the E consists of approximately 11 small, subcircular osteoderms that parallel the posterior margin of the jugal and the ventral margin of the canthal crest. The posteriormost of these is the largest and lies just dorsal to the cephalic condyle of the quadrate. The middle arm of the E consists of six small to moderately large, plate-like osteoderms extending from the midpoint of the posterior margin of the jugal to the anterodorsal corner of the quadrate. The ventral arm of the E consists of approximately three small, plate-like osteoderms that parallel the posteroventral corner of the jugal and extend posteriorly.

Only a small number osteoderms occur along the lower jaw. These include a few small, sub-circular ones lateral to the jaw near the posterior margin of the dentary, a subcircular one near the ventromedial margin of the jaw at the level of contact between the palatine and maxilla, and a few plate-like ones along the dorsolateral margin of the surangular just behind the coronoid process.

Osteoderms are limited to the dorsal and dorsolateral aspects of the neck. There is a central field of approximately six small to moderately large plate-like osteoderms just posterior to the braincase. This field is bounded by two linear series of large, plate-like osteoderms that run from the posterior margin of the squamosal posteromedially beyond the boundary of the CT dataset.

Inner Ear

The inner ear cavities of *S. crocodilurus* are described, from anterior to posterior and relative to external landmarks of the braincase, based on a digital endocast derived from FMNH 215541 (Figures 20, 21). The anterior semicircular canal emerges from the anterior ampulla of the anterior

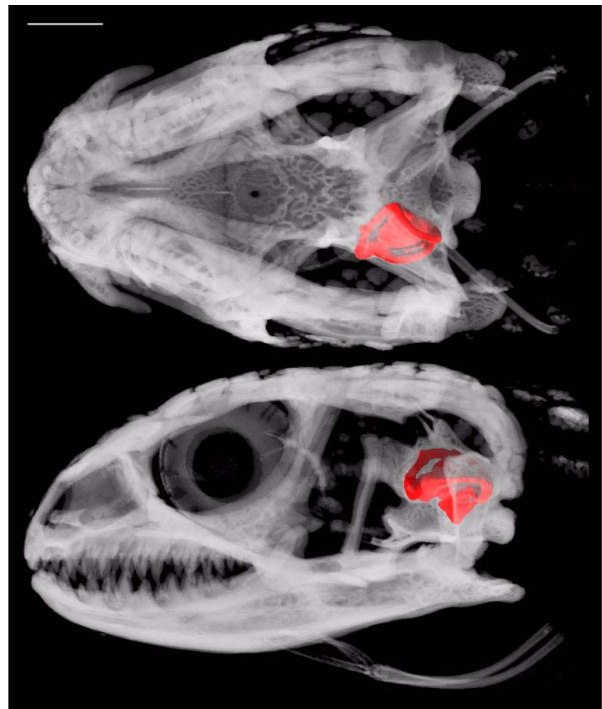


Figure 20. Digital reconstruction of the skull of an adult *S. crocodilurus* (FMNH 215541). The skull is rendered partially transparent, with the left inner ear cavity highlighted in red. Figure 21 provides an illustration of the digital endocast of the left inner ear. Top: dorsal view; bottom: left lateral view. Scale bar = 5 mm.

ampullar recess in the prootic, near the level of the origin of the basiptyergoid process. It abruptly turns posterodorsally, continuing to eventually meet the recessus crus communis in the supraoccipital. At the level of the facial foramen the anterior acoustic foramen, which transmits the anterior branch of the auditory nerve (Oelrich 1956), opens into the cranial cavity from the ventromedial wall of the anterior ampullar recess. The horizontal semicircular canal then emerges from the external ampulla of the anterior ampullar recess, continuing posteriorly to eventually meet the posterior ampullar recess in the otooccipital. The anterior ampullar recess then opens into the vestibule, which houses the statolith mass, saccule, utricle, and sinuses (Oelrich 1956).

The lagenar recess starts to differentiate from the ventral portion of the vestibule at the level of the prootic-otooccipital suture, eventually extending ventrally to the level of the base of the basal tubercle. This recess houses the lagena and perilymphatic cistern and duct (Oelrich 1956). Further posteriorly, near the dorsal-most extension of the supraoccipital, the anterior semicircular canal opens into the recessus crus communis. At the same level the endolymphatic canal and posterior acoustic foramen open into the cranial cavity from the dorsomedial and ventromedial portions of the

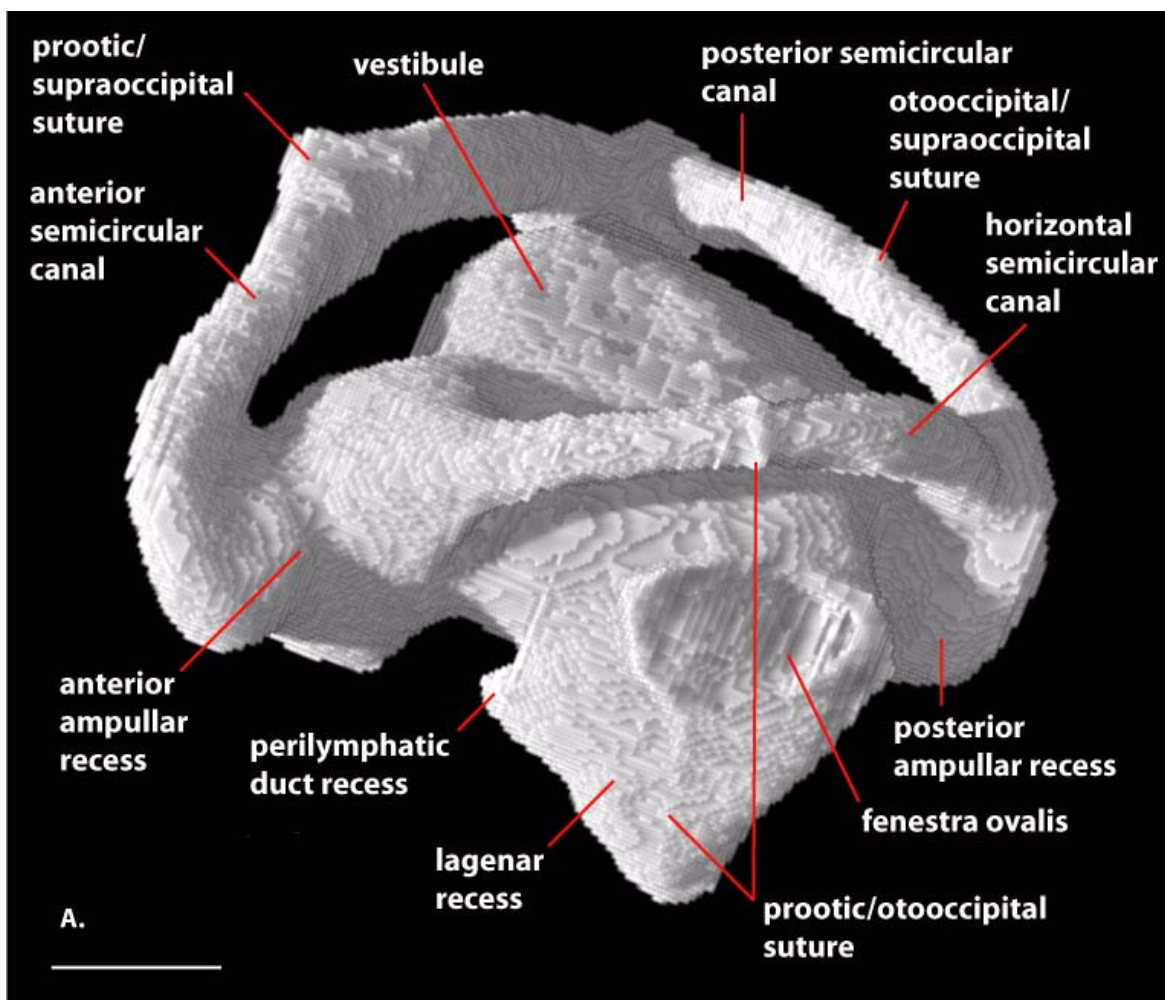


Figure 21. 3D digital endocast of the left inner ear cavities in an adult *S. crocodilurus* (FMNH 215541). A: lateral view; B: medial view. The endocast is illustrated in place in the skull in Figure 20. Scale bar = 1 mm.

vestibule, respectively; the latter transmits the posterior branch of the auditory nerve (Oelrich 1956).

The laterally facing fenestra ovalis straddles the prootic-otooccipital suture and is approximately two-thirds filled by the stapedial footplate. The posterior semicircular canal emerges from the recessus crus communis at the level of the base of the basal tubercle and continues posteroventrally to meet the posterior ampullar recess. Just posterior to the level of the recessus crus communis, the perilymphatic duct recess opens into the cranial cavity from the otooccipital via the medial aperture of the recessus scala tympani. The posterior ampullar recess starts to differentiate from the posterior end of the vestibule at the level of the stapedial footplate and is met by the posterior semicircular canal just anterior to the base of the occipital condyle.

DISCUSSION

Systematic Position and Taxonomy

The specialized morphology of *S. crocodilurus* was recognized in its original description in 1930, and for over two decades it was classified as the only known species of the family Shinisauridae. General similarities in cranial and scale characters led McDowell and Bogert (1954) to unite *S. crocodilurus* with Central American *Xenosaurus* in an expanded Xenosauridae. The differences in masticatory muscles between *S. crocodilurus* and *Xenosaurus* were discussed by Haas (1960). In an expanded treatment of the cranial myology and osteology Rieppel (1980) concluded that retention of these two taxa within Xenosauridae was the most parsimonious explanation of the available data, but that his data provided evidence of a very early split between the two.

Subsequent comparative study of the skeletal system of *S. crocodilurus* and *Xenosaurus* resulted

in a proposed resurrection of Shinisauridae, and a suggestion that its phylogenetic affinities may lie more closely with Anguidae (Hu et al. 1984). This suggestion was endorsed by Wu and Huang (1986) based on comparison of body proportions as well as similarities in the skull, mandible, vertebral column and girdles.

Many phylogenetic analyses of squamates or anguimorphs in recent years (including the influential Estes et al. [1988] paper) followed the McDowell and Bogert classification and did not analyze *S. crocodilurus* as a distinct terminal taxon. Estes et al. (1988) listed 12 synapomorphies uniting the two taxa into Xenosauridae, but some of these characters are now interpreted to be plesiomorphic or to apply to more inclusive groups of anguimorphs (Gao and Norell 1998; see also Hu et al. 1984). No consensus has emerged from the recent phylogenetic analyses that did treat the two as separate terminal taxa. Gao and Norell (1998) recovered a tree in which *Xenosaurus* and *S. crocodilurus* are each other's closest living relatives, as did Lee and Caldwell (2000). Phylogenetic analyses by Caldwell (1999) did not recover them as sister taxa, and his trees suggested a closer affinity with Anguidae (see also Hu et al. 1984). A molecular phylogeny by Macey et al. (1999) also did not recover *S. crocodilurus* and *Xenosaurus* as sister taxa, and those authors reverted to separate familial-level designation for *S. crocodilurus* (Shinisauridae). More recently, analysis of mtDNA sequence data by Wiens and Slingluff (2001) yielded a maximum-likelihood tree in which *S. crocodilurus* is basal to {*Xenosaurus* + Anguidae}. Given the recognition of phylogenetic uncertainty for *S. crocodilurus*, and the morphological disparity indicating an ancient split from *Xenosaurus* (Rieppel 1980; Wu and Huang 1986; Conrad 2004), the continued unification of the two taxa in a single family-level grouping seems ill advised and does not "make a lot of sense" (Pianka and Vitt 2003:273). At a minimum, the two taxa should be evaluated independently in future phylogenetic analyses, and it is clear that *Xenosaurus* cannot be used as a convenient morphological proxy for *S. crocodilurus* (Conrad 2004).

OBSERVATIONS ON ONTOGENETIC CHANGE

Some ontogenetic differences in the morphology and behavior of *S. crocodilurus* were noted previously by several authors, but only minimal data are available. Although both adults and juveniles will seek shelter in water when disturbed, juveniles appear to spend less time under water than adults (less than 5 minutes as opposed to from 10 to 20 minutes for adults; Zhao et al. 1999).

Ontogenetic changes in coloration were discussed by Fan (1931) and Zhao et al. (1999; see also color photos in Zhang et al. 1996). The acoustic membrane is distinct in hatchlings but is obscured by scales in older individuals. This is shown in the photos of Sprackland (1995, p. 9) and Mägdefrau (1997, p. 59). The acoustic membrane is already largely obscured in the 59.1 mm SVL individual we scanned. *Shinisaurus crocodilurus* may be unique in the transformations that take place in scale surface morphology through ontogeny (see discussion by Harvey 1993).

Preliminary observations of ontogenetic differences in the shape of the skull and of individual dermatocranial elements in *S. crocodilurus* were provided by Conrad (2004) and were based on examination of 11 specimens. Our observations of ontogenetic change in *S. crocodilurus* complement those of Conrad (2004), were derived from the examination of only four specimens (two juveniles and two adults), and are limited to the anatomical systems we investigated. There are no known previous discussions of ontogenetic changes in the braincase elements of *S. crocodilurus*, and there is a paucity of this type of information for lizards generally. Some of our observations of morphological features of the braincase in *S. crocodilurus* that undergo ontogenetic change mirror those reported for other lizards (e.g., Hikida 1978; Barahona and Barbadillo 1997, 1998; Bell et al. 2003). These features include closure of the basicranial fontanelle, increasingly tight sutural contact between elements (initially the elements are separated from one another by cartilaginous growth zones, but these subsequently form sutural contacts and eventually may fuse in large adults), and changes in the relative prominence or size of foramina and canals (e.g., anterior abducens foramen and semicircular canals).

In at least some lizards, the orbitosphenoids are not ossified in early stages of postnatal ontogeny (Barahona and Barbadillo 1998). They are present and ossified as flattened ovoid elements in TNHC 62987 but are elongated bones in FMNH 215541. In the adult, some of the surrounding cartilages are also heavily calcified and, thus, appear in the CT data sets. In iguanines the orbitosphenoid bones become increasingly complex as ossification proceeds along orbital cartilages (de Queiroz 1987), but the range of morphological variation through ontogeny in *S. crocodilurus* is unknown (the two CT specimens are the only specimens in which the orbitosphenoids are described).

As a result of increasing ossification, the overall shape of the sphenoid changes through ontogeny in *S. crocodilurus*. This is most evident in

views of the height of the dorsum sella (Figure 3G, H) and in lateral view where the ventral margin becomes more strongly curved in the adult (Figure 3E, F). The finger-like secondary processes on the basioccipital processes of the juvenile (Figure 4) are reduced or lost in the adult. The basipterygoid processes show a greater expansion at their distal ends in the adult, similar to that documented for some lacertid and gymnophthalmid species (Barahona and Barbadillo 1997, 1998; Bell et al. 2003). Distinct mineralized distal tips of those processes are evident in the adult CT images (Figure 8) but are absent in the juvenile data set, which reveals that the distal ends are poorly ossified. Increased calcification/ossification at the distal ends of these processes was also reported for lacertid lizards (Barahona and Barbadillo 1998).

The most pronounced ontogenetic change in the basioccipital is the increased development of the basal tubera. In the adult CT data set distinct ossifications are visible at the ventral margins of the tubera. These changes also were reported for some lacertids and skinks (Hikida 1978; Barahona and Barbadillo 1998). In *S. crocodilurus* the occipital condyle is less prominent in the juvenile, and the relative contribution of the basioccipital to the condyle increases through ontogeny (Figure 11, J).

The supraoccipital is anteroposteriorly shortened in the juvenile relative to the adult (Figure 10A-D). As is true for other lizards (Barahona and Barbadillo 1997, 1998), the cartilaginous process ascendens of the supraoccipital in *S. crocodilurus* is not calcified in the juvenile. The dorsal crest is not well developed in either specimen we scanned, but it rises higher above the posterior surface of the bone in the adult. The foramen magnum and posterior cranial cavity form a smooth arch with straight vertical sides in the juvenile, but become constricted by ossification of the medial wall of the otic chamber in the adult (Figure 10G, H). Calcified endolymph is much more extensively developed in the juvenile than in the adult, supporting the hypothesis that endolymph reserves are utilized for skeletal growth in early postnatal ontogeny (e.g., Packard et al. 1985; Kluge 1987; see also the discussion by Bauer 1989).

The alar process of the prootic is well developed in the adult, but absent in the juvenile (also reported for lacertids by Barahona and Barbadillo 1997, 1998). As a consequence, the anteroposterior extent of the incisura prootica increases through ontogeny. The crista prootica also is not developed in the juvenile, so the facial foramen is exposed in lateral view (Figure 12H). The acoustic recess in the juvenile contains two foramina, one

for the facial foramen and a single large foramen for the eighth cranial nerve (instead of two foramina for VIII seen in the adult). This decreased number of foramina in the acoustic recess contrasts with an increased number (four) reported in juveniles of the lacertid *Gallotia galloti* (Barahona and Barbadillo 1998).

The paroccipital process of the otooccipital in *S. crocodilurus* and other lizards is weakly developed in the juvenile (Barahona and Barbadillo 1997, 1998). In the *S. crocodilurus* adult the lateral edge of the paroccipital process bears a dorsally oriented process that is absent in the juvenile. The perilymphatic foramen in the juvenile is not entirely enclosed by bone as it is in the adult.

Cephalic osteoderms are well developed in the adult (Figure 18) but are absent in the juvenile. Ontogenetic differences in the presence of cephalic osteoderms were also discussed by Barahona and Barbadillo (1997).

SUMMARY AND CONCLUSIONS

The braincase long has been considered a rich source of data by vertebrate morphologists interested in testing hypotheses of evolutionary relationships and studying the complex relationship between the skeletal and nervous systems. The number of taxa for which detailed descriptions of braincase anatomy are available, however, does not come close to accurately reflecting the taxonomic diversity within most vertebrate groups. One reason for this disparity is that the study of internal cranial anatomy largely is a destructive process and therefore logistically difficult for rare taxa that are not well represented in museum collections.

We utilized X-ray computed tomography as a non-destructive technique for visualizing and describing the braincase of the rare, anguimorph lizard, *Shinisaurus crocodilurus*, which today is known to inhabit only portions of southeastern China and northeastern Vietnam. In addition to revealing internal details of the braincase elements, computed tomography allowed us to provide the first description of the cranial osteoderms and inner ear cavities of this lizard. Our examination of both juvenile and adult specimens of *S. crocodilurus* emphasizes the need for increased understanding of both individual and ontogenetic variation in anguimorph cranial osteology and systematics. The hope is that our observations and the digital images generated in this study will represent a valuable source of data for both current and future morphologists and systematists with an interest in squamate reptiles.

A TRIBUTE TO WILL DOWNS

When we began this project, we were immediately confronted with the challenge of obtaining and translating the Chinese literature on *Shinisaurus*. Following a brief explanation of our problem during a conversation with Will, Bell received a prompt response that Will was willing to assist. He quickly provided a translation of the osteology section of Zhang (1991), but then refused to accept the payment previously agreed upon for his translation services. Instead, he said that it “seemed like an interesting animal” and it was payment enough to be able to learn a little more about it. Over the next several months Will translated the entire section on *S. crocodilurus* from Zhao et al. (1999), and provided translations of Hu et al. (1984) and Wu and Huang (1986) for this project. Two of these translations were posted, along with others prepared by Will, on the Polyglot Paleontologist web site (<http://ravenel.si.edu/paleo/paleoglot/index.cfm>). His translations also were utilized in at least two other anatomical studies on *S. crocodilurus* (Conrad 2004), and are available now for the paleontological and zoological researchers interested in this most unusual species. Among paleontologists, Will’s linguistic abilities are perhaps best known and appreciated through his translations of papers on Asian fossil mammals and stratigraphy. We are pleased to acknowledge his contribution to the herpetology community! Will, like so many of us, was a student of Life, and his enthusiastic willingness to apply his skills for the benefit of his colleagues and friends was widely appreciated.

ACKNOWLEDGMENTS

Because of their nature, literature compilations often are not acknowledged or cited, but our efforts to understand the biology and anatomy of *S. crocodilurus* were greatly facilitated by the invaluable compilation by Zhao and Zhao (1994). That source led us to many papers difficult to obtain in the United States, and our ability to acquire them was made possible by assistance from B. Bartholomew, J. Mead, D. Trombatore, and E.-m. Zhao. Their efforts on our behalf are gratefully acknowledged. Translation assistance from W. Downs and Z.-I. Yang was most helpful. S. Evans generously provided the juvenile specimen we scanned, and, through years of conversation and patience, helped us to better understand the intricacies of the lizard skull. Loans of additional specimens utilized in this project were facilitated by J. Mead (NAU), A. Resetar (FMNH), B. Stein (MVZ), and J. Vindum

(CAS). HRXCT scanning was performed by R. Ketcham and M. Colbert (they always make it look so easy!). A. Balanoff graciously donated her time in helping with image processing and digital data manipulations. J. Head and M. Polcyn improved this paper with their reviews. We also thank L. Jacobs and L. Taylor for their editorial assistance. Financial support for this research was received from the Geology Foundation at the University of Texas, and from the National Science Foundation (NSF-EF-033-4961).

REFERENCES

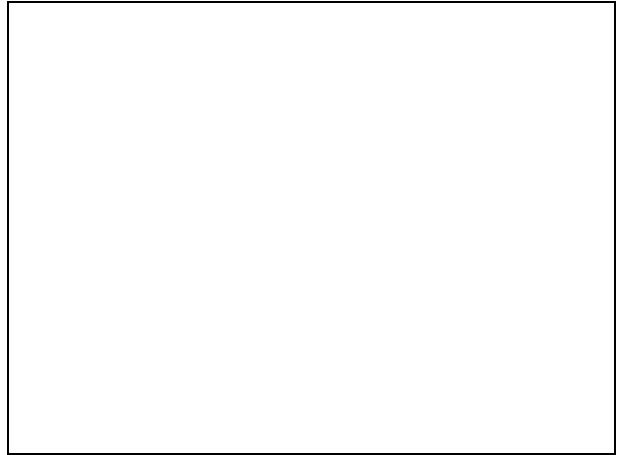
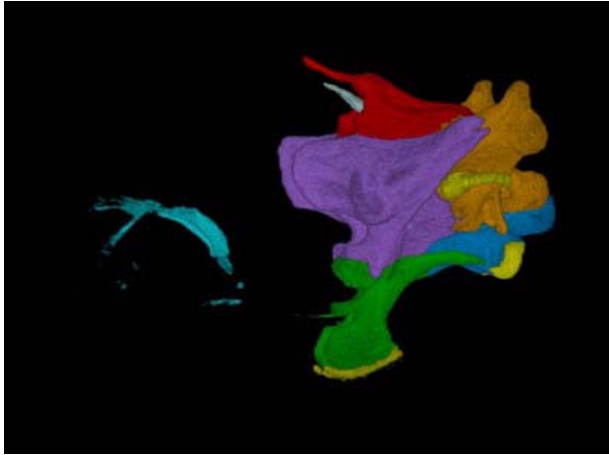
- Alifanov, V.R. 2000. The fossil record of Cretaceous lizards from Mongolia, p. 368-389. In Benton, M.J., Shishkin, M.A., Unwin, D.M., and Kurochkin, E.N. (eds.), *The Age of Dinosaurs in Russia and Mongolia*. Cambridge University Press, New York.
- Barahona, F. and Barbadillo, L.J. 1997. Identification of some Iberian lacertids using skull characters. *Revista Española de Herpetología*, 11:47-62.
- Barahona, F. and Barbadillo, L.J. 1998. Inter- and intraspecific variation in the post-natal skull of some lacertid lizards. *Journal of Zoology (London)*, 245:393-405.
- Bauer, A.M. 1989. Extracranial endolymphatic sacs in *Eurydactylodes* (Reptilia: Gekkonidae), with comments on endolymphatic function in lizards. *Journal of Herpetology*, 23:172-175.
- Bell, C.J., Evans, S.E., and Maisano, J.A. 2003. The skull of the gymnophthalmid lizard *Neusticurus ecleopus* (Reptilia: Squamata). *Zoological Journal of the Linnean Society*, 139:382-304.
- Bellairs, A.d'A. and Kamal, A.M. 1981. The chondrocranium and the development of the skull in recent reptiles, p. 1-283. In Gans, C. and Parsons, T.S. (eds.), *Biology of the Reptilia, Volume 11, Morphology F.*, Academic Press, New York.
- Böhme, W. 1988. Zur Genitalmorphologie der Sauria: Funktionelle und Stammesgeschichtliche Aspekte. *Bonner Zoologische Monographien*, 27:1-176.
- Borsuk-Bialynicka, M. 1985. Carolinidae, a new family of xenosaurid-like lizards from the Upper Cretaceous of Mongolia. *Acta Palaeontologica Polonica*, 30:151-176, Plates 1-4.
- Borsuk-Bialynicka, M. 1986. On the diagnosis of the Xenosauridae (Anguimorpha), p. 213-217. In Rocek, Z. (ed.), *Studies in Herpetology: Proceedings of the European Herpetological Meeting (3rd Ordinary General Meeting of the Societas Europaea Herpetologica)*, Prague 1985. Charles University, Prague.
- Borsuk-Bialynicka, M. 1987. *Carusia*, a new name for the Late Cretaceous lizard *Carolina* Borsuk-Bialynicka, 1985. *Acta Palaeontologica Polonica*, 32:151.
- Borsuk-Bialynicka, M. 1991a. Cretaceous lizard occurrences in Mongolia. *Cretaceous Research*, 12:607-608.

- Borsuk-Bialynicka, M. 1991b. Questions and controversies about saurian phylogeny, Mongolian perspective, p. 9-10. In Kielan-Jaworowska, Z., Heintz, N., and Nakrem, H.A. (eds.), *Fifth Symposium on Mesozoic Terrestrial Ecosystems and Biota, Extended Abstracts*. Contributions from the Paleontological Museum, University of Oslo 364.
- Caldwell, M.W. 1999. Squamate phylogeny and the relationships of snakes and mosasauroids. *Zoological Journal of the Linnean Society*, 125:115-147.
- Conrad, J.L. 2002. First fossil relative of *Shinisaurus* (Anguimorpha, Squamata) and the phylogenetic importance of Shinisauridae. *Journal of Vertebrate Paleontology*, 22(Supplement to 3):46A.
- Conrad, J.L. 2004. Skull, mandible, and hyoid of *Shinisaurus crocodilurus* Ahl (Squamata, Anguimorpha). *Zoological Journal of the Linnean Society*, 141:399-434.
- Costelli, J., Jr. and Hecht, M.K. 1971. The postcranial osteology of the lizard *Shinisaurus*: the appendicular skeleton. *Herpetologica*, 27:87-98.
- de Queiroz, K. 1987. Phylogenetic systematics of iguaine lizards: A comparative osteological study. *University of California Publications in Zoology*, 118:1-203.
- Estes, R., de Queiroz, K., and Gauthier, J. 1988. Phylogenetic relationships within Squamata, p. 119-281. In Estes, R. and Pregill, G. (eds.), *Phylogenetic Relationships of the Lizard Families: Essays Commemorating Charles L. Camp*. Stanford University Press, Stanford, California.
- Evans, H.E. 1993. The skeleton, p. 122-218. In Evans, H.E. (ed.), *Miller's Anatomy of the Dog, Third Edition*. W.B. Saunders Company, Philadelphia.
- Fan, T.H. 1931. Preliminary report of reptiles from Yaoshan, Kwangsi, China. *Bulletin of the Department of Biology, College of Science, Sun Yatsen University*, 11:1-154.
- Gao, K. and Hou, L. 1996. Systematics and taxonomic diversity of squamates from the Upper Cretaceous Djadochta Formation, Bayan Mandahu, Gobi Desert, People's Republic of China. *Canadian Journal of Earth Sciences*, 33:578-598.
- Gao, K.-q. and Nessov, L.A. 1998. Early Cretaceous squamates from the Kyzylkum Desert, Uzbekistan. *Neues Jahrbuch für Geologie und Paläontologie Abhandlungen*, 207:289-309.
- Gao, K.-q. and Norell, M.A. 1998. Taxonomic revision of *Carusia* (Reptilia: Squamata) from the Late Cretaceous of the Gobi Desert and phylogenetic relationships of anguimorph lizard. *American Museum Novitates*, 3230:1-51.
- Gauthier, J.A. 1982. Fossil xenosaurid and anguid lizards from the early Eocene Wasatch Formation, southeast Wyoming, and a revision of the Anguioidea. *Contributions to Geology, University of Wyoming*, 21:7-54.
- Gritis, P. 1990. Observations on the lizard *Shinisaurus crocodilurus* in captivity. *Herpetological Review*, 21:81-83.
- Grychta, U. 1993. *Shinisaurus crocodilurus* Ahl, 1930 – Haltung, Ernährung, Geburt und neue Erkenntnisse über die Krokodilschwanzhöckerechse. *Sauria*, 15:9-10.
- Haas, G. 1960. On the trigeminus muscles of the lizards *Xenosaurus grandis* and *Shinisaurus crocodilurus*. *American Museum Novitates*, 2017:1-54.
- Haas, G. 1973. Muscles of the jaws and associated structures in the Rhynchocephalia and Squamata, p. 285-490. In Gans, C. and Parsons, T.S. (eds.), *Biology of the Reptilia, Volume 4, Morphology D.*, Academic Press, New York.
- Harvey, M.B. 1993. Microstructure, ontogeny, and evolution of scale surfaces in xenosaurid lizards. *Journal of Morphology*, 216:161-177.
- Hecht, M.K. and Costelli, J. Jr. 1969. The postcranial osteology of the lizard *Shinisaurus*. 1. The vertebral column. *American Museum Novitates*, 2378:1-21.
- Hikida, T. 1978. Postembryonic development of the skull of the Japanese skink, *Eumeces latiscutatus* (Scincidae). *Japanese Journal of Herpetology*, 7:56-72.
- Hofmann, E.G. 2000. The Chinese crocodile lizard (*Shinisaurus crocodilurus*): mysterious slumberer of the Mogots. *Reptiles Magazine*, 8(4):60, 62-71.
- Hu, Q.-x. 1980. [The anatomy of the nervous system of *Shinisaurus crocodilurus* Ahl (Reptilia: Sauria)]. *Acta Herpetologica Sinica (Chengdu), old series*, 4(2):1-11. [In Chinese].
- Hu, Q.-x., Jiang, Y.-m., and Zhao, E.-m. 1984. [A study on the taxonomic status of *Shinisaurus crocodilurus*]. *Acta Herpetologica Sinica*, 3:1-7. [In Chinese, with English summary].
- Huang, Q. 1992. [The anatomy of the muscular systems of *Shinisaurus crocodilurus* (Lacertilia: Shinisauridae), p. 47-66. In Jiang, Y.-m. (ed.), *A Collection of Papers on Herpetology*. Sichuan Scientific and Technical Publishing House, Chengdu.
- Jollie, M.T. 1960. The head skeleton of the lizard. *Acta Zoologica*, 41:1-64.
- Kluge, A.G. 1987. Cladistic relationships in the Gekkonoidea (Squamata, Sauria). *University of Michigan Museum of Zoology Miscellaneous Publications*, 173:1-54.
- Kudrjawtsew, S.W. and Wasiljew, D.B. 1991. Haltung und Zucht der Krokodilschwanz-Höckerechse *Shinisaurus crocodilurus* Ahl, 1930 im Moskauer Zoo. *Salamandra*, 27:219-221.
- Kudryavtsev, S.V. and Vassilyev, D.B. 1998. Reproduction of *Shinisaurus crocodilurus* Ahl., 1930 at the Moscow Zoo. *Russian Journal of Herpetology*, 5:15-16.
- Lee, M.S.Y. and Caldwell, M. 2000. *Adriosaurus* and the affinities of mosasaurs, dolichosaurs, and snakes. *Journal of Paleontology*, 74:915-937.
- Li, J.-f. and Wu, Q.-j. 1988. [Study on the optic nerve of *Shinisaurus crocodilurus*]. *Acta Zoologica Sinica (Beijing)*, 34:88-90. [In Chinese].
- Li, J.-l. 1991. [Fossil reptiles from Zhaili Member, Hedi Formation, Yuanqu, Shanxi]. *Vertebrata Palasiatica*, 29:276-285. [In Chinese, with English summary].

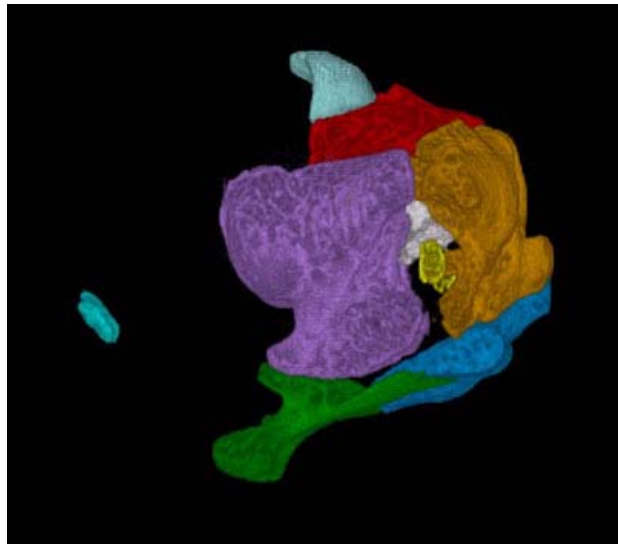
- Macey, J.R., Schulte, J.A. II, Larson, A., Tuniyev, B.S., Orlov, N., and Papenfuss, T.J. 1999. Molecular phylogenetics, tRNA evolution, and historical biogeography in anguid lizards and related taxonomic families. *Molecular Phylogenetics and Evolution*, 12:250-272.
- Mägdefrau, H. 1987. Zur Situation der Chinesischen Krokodilschwanz-Höckerechse, *Shinisaurus crocodilurus* Ahl, 1930. *Herpetofauna*, 9(51):6-11.
- Mägdefrau, H. 1997. Biologie, Haltung und Zucht der Krokodilschwanz-Höckerechse (*Shinisaurus crocodilurus*). *Zeitschrift des Kölner Zoo*, 40:55-60.
- Maisano, J.A. 2001. A survey of state of ossification in neonatal squamates. *Herpetological Monographs*, 15:135-157.
- Maisano, J.A. 2002. Postnatal skeletal ontogeny in five xantusiids (Squamata: Scleroglossa). *Journal of Morphology*, 254:1-38.
- McDowell, S.B., Jr. and Bogert, C.M. 1954. The systematic position of *Lanthanotus* and the affinities of the anguimorph lizards. *Bulletin of the American Museum of Natural History*, 105:1-142, Plates 1-16.
- Nessov, L.A. and Gao, K. 1993. Cretaceous lizards from the Kizylkum Desert, Uzbekistan. *Journal of Vertebrate Paleontology*, 13 (Supplement to 3):51A.
- Norell, M.A. and Gao, K. 1997. Braincase and phylogenetic relationships of *Estesia mongoliensis* from the Late Cretaceous of the Gobi Desert and the recognition of a new clade of lizards. *American Museum Novitates*, 3211:1-25.
- Oelrich, T.M. 1956. The anatomy of the head of *Ctenosaura pectinata* (Iguanidae). *Miscellaneous Publications, Museum of Zoology, University of Michigan*, 94:1-122, Figures 1-59.
- Packard, M.J., Packard, G.C., Miller, J.D., Jones, M.E., and Gutzke, W.H.N. 1985. Calcium mobilization, water balance, and growth in embryos of the agamid lizard *Amphibolurus barbatus*. *Journal of Experimental Zoology*, 235:349-357.
- Pianka, E.R. and Vitt, L.J. 2003. *Lizards: Windows to the Evolution of Diversity*. University of California Press, Berkeley, California.
- Quyet, L.K. and Ziegler, T. 2003. First record of the Chinese crocodile lizard from outside of China: Report on a population of *Shinisaurus crocodilurus* Ahl, 1930 from north-eastern Vietnam. *Hamadryad*, 27:193-199.
- Rieppel, O. 1980. The phylogeny of anguimorph lizards. *Denkschriften der Schweizerischen Naturforschenden Gesellschaft*, 94:1-86.
- Rieppel, O. 1992. Studies on skeletal formation in reptiles. III. Patterns of ossification in the skeleton of *Lacerta vivipara* Jacquin (Reptilia, Squamata). *Fieldiana: Zoology, n.s.*, 68:1-25.
- Rieppel, O. 1993. Patterns of diversity in the reptilian skull, p. 344-390. In Hanken, J. and Hall, B.K. (eds.), *The Skull, Volume 2: Patterns of Structural and Systematic Diversity*. University of Chicago Press.
- Rieppel, O. and Zaher, H. 2000. The braincases of mosasaurs and *Varanus*, and the relationships of snakes. *Zoological Journal of the Linnean Society*, 129:489-514.
- Säve-Söderbergh, G. 1947. Notes on the brain-case in *Sphenodon* and certain Lacertilia. *Zoologiska Bidrag från Uppsala*, 25:489-516.
- Shen, L.-t. and Li, H.-h. 1982. [Notes on the distribution and habits of the lizard *Shinisaurus crocodilurus* Ahl]. *Acta Herpetologica Sinica*, 1(1):84-85. [In Chinese].
- Shen, L.-t. and Li, H.-h. 1987. Notes on the distribution and habits of the lizard *Shinisaurus crocodilurus* Ahl. *Bulletin of the Chicago Herpetological Society*, 22:4-5. [English translation of Shen and Li 1982].
- Sprackland, R.G. 1989. An enigmatic dragon brought to light; the Chinese crocodile lizard in captivity. *Shinisaurus crocodilurus*. *The Vivarium*, 2(2):12-14, 23-24.
- Sprackland, R.G. 1993. The biology of the Chinese crocodile lizard in captivity, p. 45-53. In Staub, R.E. (ed.), *Proceedings of the Northern California Herpetological Society's 1991 Conference on Captive Propagation and Husbandry of Reptiles and Amphibians*. Northern California Herpetological Society, Davis, California. [Reprinted essentially verbatim in Sprackland 1995].
- Sprackland, R.G. 1995. The biology of the Chinese crocodile lizard in captivity. *The Reptilian*, 4(2):9-15.
- Thatcher, T. 1990. The Chinese crocodile lizard, *Shinisaurus crocodilurus*, notes on captive births and husbandry. *British Herpetological Bulletin*, 33:17-19.
- Underwood, G. 1957. *Lanthanotus* and the anguimorph lizards: A critical review. *Copeia*, 1957:20-30.
- Underwood, G. 1970. The eye, p. 1-97. In Gans, C. and Parsons, T.S. (eds.), *Biology of the Reptilia, Volume 2, Morphology B*. Academic Press, New York.
- Wei, Y.-n., Zhang, Y.-x., and Tang, Z.-j. 2000. [Analysis and comparison of gel electrophoresis of soluble proteins in the serum skeletal muscle and liver of *Shinisaurus crocodilurus* Ahl]. *Cultum Herpetologica Sinica*, 8:273-275. [In Chinese].
- Wever, E. G. 1978. *The Reptile Ear: Its Structure and Function*. Princeton University Press, Princeton.
- Wiens, J. J., and Slingluff, J. L. 2001. How lizards turn into snakes: A phylogenetic analysis of body-form evolution in anguid lizards. *Evolution*, 55:2303-2318.
- Wilke, H. 1985. Krokodilschwanz-Höckerechsen im Vivarium Darmstadt. *Die Aquarien- und Terrarien-Zeitschrift*, 38:234.
- Wilke, H. 1987. Crocodile-tailed knobby lizards in the Darmstadt Vivarium. *Bulletin of the Chicago Herpetological Society*, 22:6.
- Wu, C.-h. and Huang, Z.-j. 1986. [A comparison of the external characters and the skeletal system between *Shinisaurus crocodilurus* and *Xenosaurus grandis*]. *Sinozoologica*, 4:41-50. [In Chinese].
- Zeng, Z.-f. and Zhang, Y.-x. 2002. [Studies on morphological variation and hibernation of *Shinisaurus crocodilurus*]. *Herpetologica Sinica*, 9:127-130. [In Chinese].
- Zhang, F.-j. 1986. [Studies of morphological characters of hemipenes of the Chinese lizard]. *Acta Herpetologica Sinica*, 5(4):254-259.

- Zhang, S.-d. and Cao, Y.-r. 1984a. [The anatomy of *Shinisaurus crocodilurus* Ahl]. *Chinese Wildlife, Harbin*, 1984(1):28-33. [In Chinese]. (Not seen; as cited in Zhao and Zhao 1994).
- Zhang, S.-d. and Cao, Y.-r. 1984b. [The anatomy of *Shinisaurus crocodilurus* Ahl]. *Chinese Wildlife, Harbin*, 1984(2):22-27. [In Chinese]. (Not seen; as cited in Zhao and Zhao 1994).
- Zhang, Y.-x. 1982. [A gross anatomy of the digestive and urogenital system of the lizard *Shinisaurus crocodilurus* Ahl]. *Acta Herpetologica Sinica*, 1(1):86-87. [In Chinese].
- Zhang, Y.-x. 1991. [*Shinisaurus: the Chinese crocodylian lizard*]. China Forestry Publishing House. [In Chinese].
- Zhang, Y.-x. and Tang, Z.-j. 1985. [The biology of *Shinisaurus crocodilurus*]. *Acta Herpetologica Sinica*, 4:337-340. [In Chinese].
- Zhang, Y.-x. and Zeng, S.-f. 2002. [Status and conservation of *Shinisaurus crocodilurus*]. *Herpetologica Sinica*, 9:186-189. [In Chinese].
- Zhang, Y.-x., Ban, R.-x., Wu, C.-m., and Chen, Z.-j. 1996. [*Studies on ultrastructure and karyotypes of crocodylian lizard*]. China Guangxi Teacher's University Press. [In Chinese].
- Zhao, E.-m. and Adler, K. 1993. *Herpetology of China*. Contributions to Herpetology, Number 10. Society for the Study of Amphibians and Reptiles, Oxford, Ohio.
- Zhao, E.-m. and Zhao, H. 1994. *Chinese Herpetological Literature: Catalogue and Indices*. Publishing House of the Chengdu University of Science and Technology, Chengdu.
- Zhao, E.-m., Li, S.-q., and Shen, Y. 1980. [The electrophoretogram of isoenzymes of lactic dehydrogenase in the liver and kidney of *Shinisaurus crocodilurus* Ahl (Reptilia: Sauria)]. *Acta Herpetologica Sinica (Chengdu), old series*, 4(1):1-3. [In Chinese].
- Zhao, E.-m., Zhao, K.-t., and Zhou, K.-y. 1999. [*Fauna Sinica, Reptilia Vol. 2: Squamata, Lacertilia*]. Science Press, Beijing. [In Chinese].
- Ziegler, T. and Böhme, W. 1997. Genitalstrukturen und Paarungsbiologie bei squamaten Reptilien, speziell den Platynta, mit Bemerkungen zur Systematik. *Mertensiella*, 8:1-210.

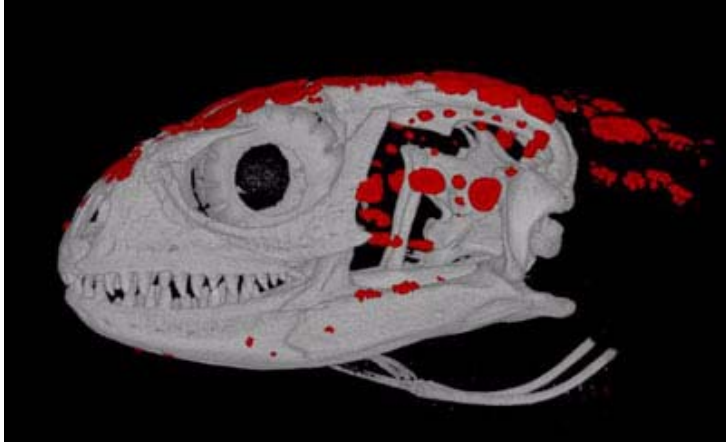
Appendix 1. Rotation of the articulated adult braincase of *S. crocodilurus* (FMNH 215541). Click to run movie.



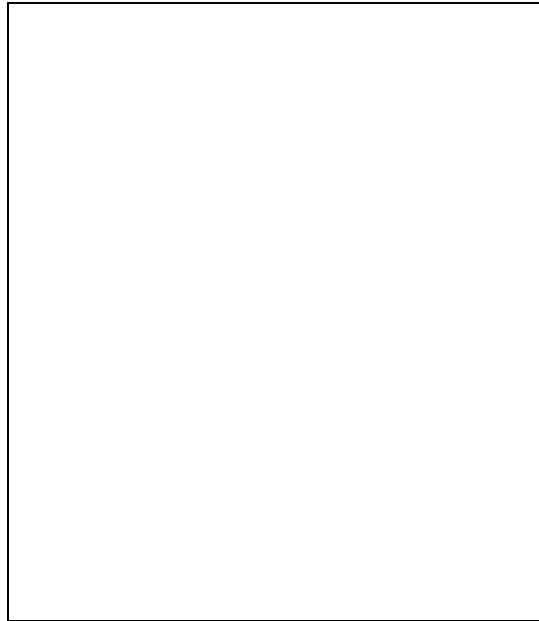
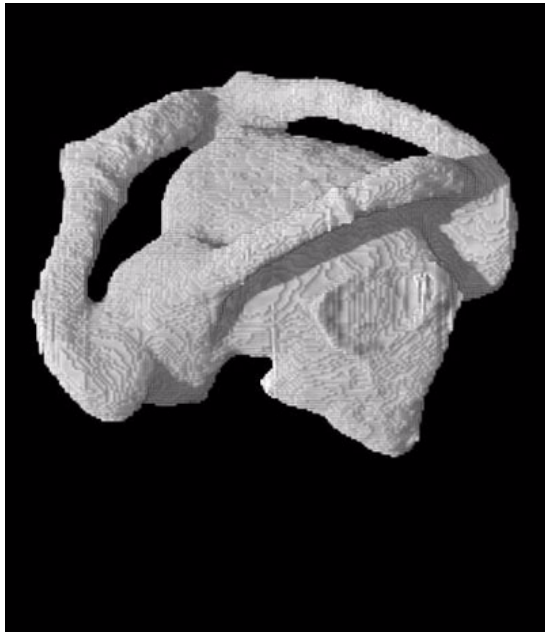
Appendix 2. Rotation of the articulated juvenile braincase of *S. crocodilurus* (TNHC 62987). Click to run movie.



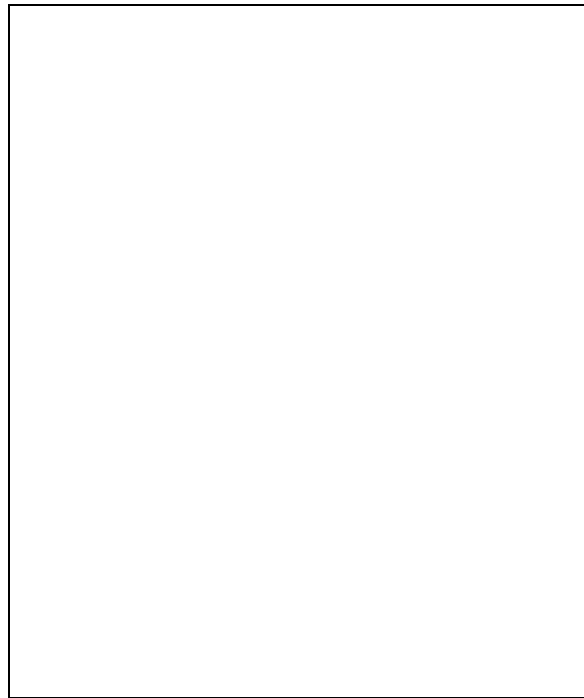
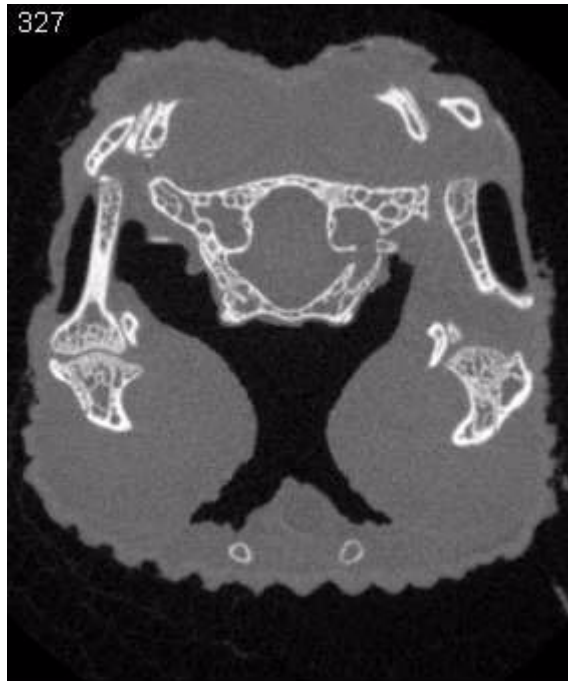
Appendix 3. Rotation of the skull and associated osteoderms of an adult *S. crocodilurus* (FMNH 215541). Click to run movie.



Appendix 4. Rotation of the digital endocast of the left inner ear cavities in an adult *S. crocodilurus* (FMNH 215541).
Click to run movie.



Appendix 5. Slice-by-slice animations along the coronal axis of the skull in an adult *S. crocodilurus* (FMNH 215541).
Click to run movie.



Appendix 6. Slice-by-slice animations along the coronal axis of the skull in a juvenile *S. crocodilurus* (TNHC 62987).
Click to run movie.

